SIEMENS

Imaging Life

The Magazine for Molecular Imaging Innovation

Clinical Case Supplement | Cardiology Edition

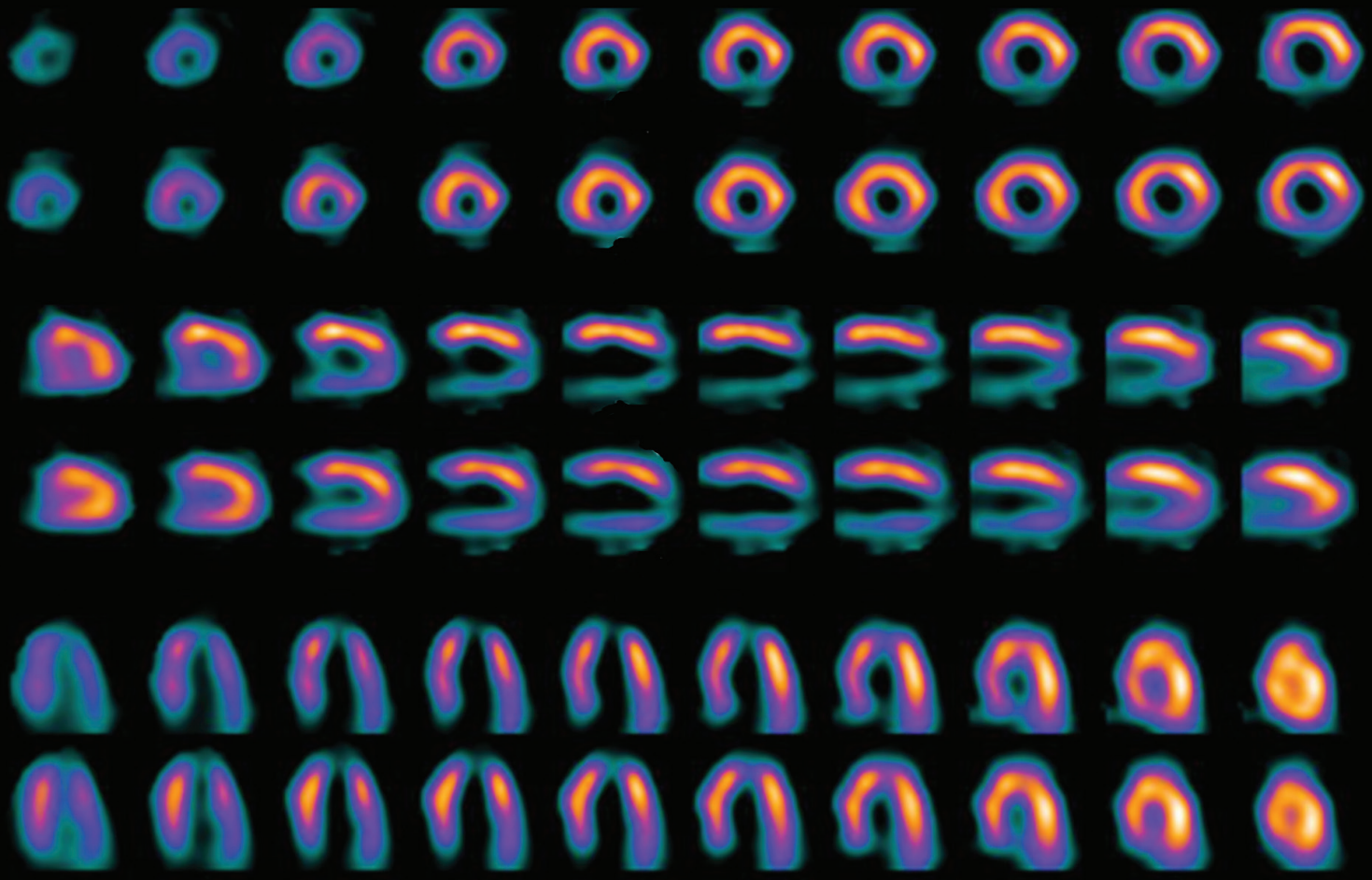

Table of Contents

Clinical Results

Case 1

Antagonistic Effect of Caffeine Ingestion on Myocardial Blood Flow Determined by ^{82}Rb Dynamic Cardiac PET/CT

By Parthiban Arumugam, MD

Data courtesy of the Department of Nuclear Medicine, Central Manchester University Hospitals, Manchester, United Kingdom

History

A 59-year-old male who had multiple risk factors for coronary artery disease (CAD)—including hypertension, hyperlipidemia and high body mass index (BMI)—presented with occasional dyspnea on exertion. In view of the intermediate likelihood for CAD, he underwent an ^{82}Rb dynamic PET/CT myocardial perfusion study, performed on Biograph™ mCT.

Following a low-dose CT for attenuation correction, a dynamic ^{82}Rb PET myocardial perfusion study was performed during rest and following adenosine stress. Immediately following the start of the IV infusion (30 mCi [1070 MBq] ^{82}Rb), list mode acquisition began. For both stress and rest studies, the gated list-mode acquisition continued for 7 minutes. Dynamic data was evaluated in *syngo*®.MBF to calculate myocardial blood flow (MBF). Summed gated stress and rest data were also evaluated in QGS/QPS, which provided a visual assessment of perfusion, stress and rest left ventricle (LV) function.

The patient denied ingesting any caffeine-containing beverages for at least 12 hours prior to the study. There were no side effects during or after adenosine stress.

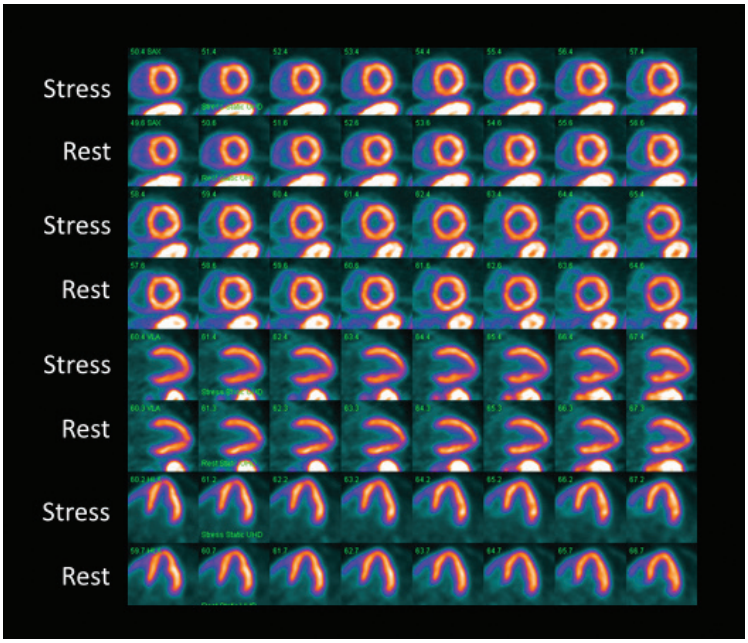

Figure 1: Summed non-gated views of stress/rest ^{82}Rb PET myocardial perfusion study show normal perfusion throughout the LV during both stress and rest.

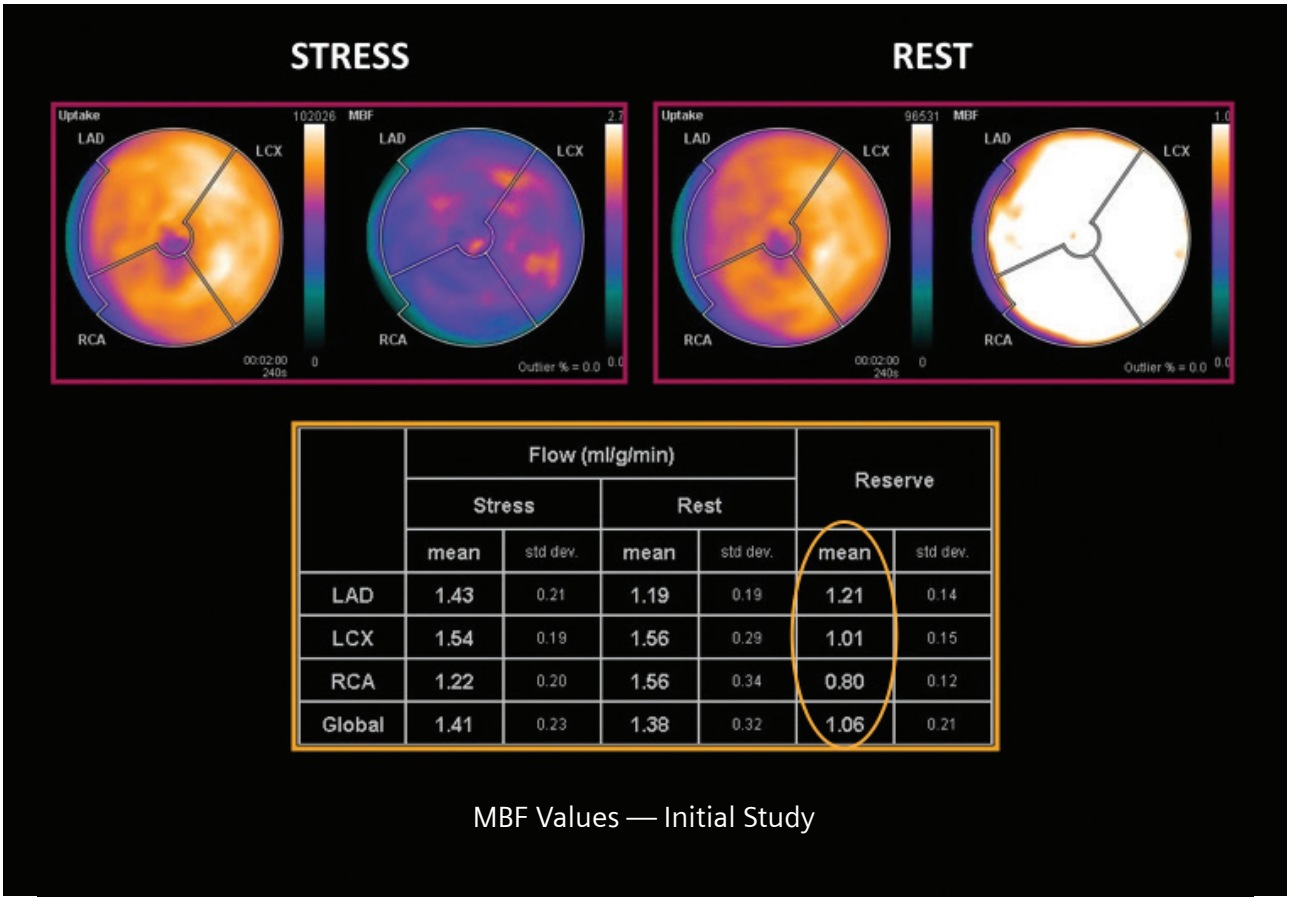

	Flow (ml/g/min)				Reserve	
	Stress		Rest			
	mean	std dev.	mean	std dev.	mean	std dev.
LAD	1.43	0.21	1.19	0.19	1.21	0.14
LCX	1.54	0.19	1.56	0.29	1.01	0.15
RCA	1.22	0.20	1.56	0.34	0.80	0.12
Global	1.41	0.23	1.38	0.32	1.06	0.21

Figure 2: MBF values show no significant response to adenosine vasodilation as demonstrated in the stress MBF values, with normal blood flow values at rest and reduced global MFR.

Diagnosis

Stress/rest ^{82}Rb PET perfusion images showed a normal sized LV, with homogenous distribution of tracer throughout the entire LV myocardium both in stress and rest—suggesting normal perfusion, no evidence of stress-induced cavity dilation or right ventricle (RV) prominence at peak stress. The LV cavity size appeared normal with mild myocardial hypertrophy reflecting hypertension and ventricular function. The ejection fraction was within normal limits. However, MBF values showed a global decrease of MBF at peak stress. The mean stress MBF in the left anterior descending (LAD) territory was 1.43 ml/gm/min, while the lower limit of normal at peak stress is 2.5 ml/gm/min. The resting MBF, however, was normal throughout the LV myocardium. Consequently, the myocardial flow reserve (MFR) values for all arterial territories were significantly lower than normal. The global decrease in stress MBF and low MFR is often associated with balanced ischemia, usually related to triple vessel disease. But, the overall normal uptake pattern, the absence of other markers of multi-vessel disease (transient ischemic dilatation [TID], RV prominence at peak stress) and the normal resting blood flow values all made the suggestion of multi-vessel disease doubtful.

Another possibility was that the patient had ingested caffeine-containing beverages within 12 hours prior to the study, which may cause inadequate vasodilatation with adenosine stress and may explain this low global stress MBF. However, since the patient had denied any caffeine intake, it was not possible to confirm the cause of the low-stress MBF. Since the pattern of uptake was not reflective of advanced CAD with balanced disease, the patient was asked to come another day for a repeat ^{82}Rb dynamic PET myocardial perfusion study. The patient was given strict instructions to avoid any caffeine for more than 12 hours prior to the PET/CT study.

The repeat study with strict adherence to restrictions on caffeine intake showed completely different stress MBF values (*Figure 3*). The stress MBF was slightly higher than the normal throughout the entire LV myocardium. The resting MBF values were normal and very similar to the values obtained in the initial study. Mean stress MBF

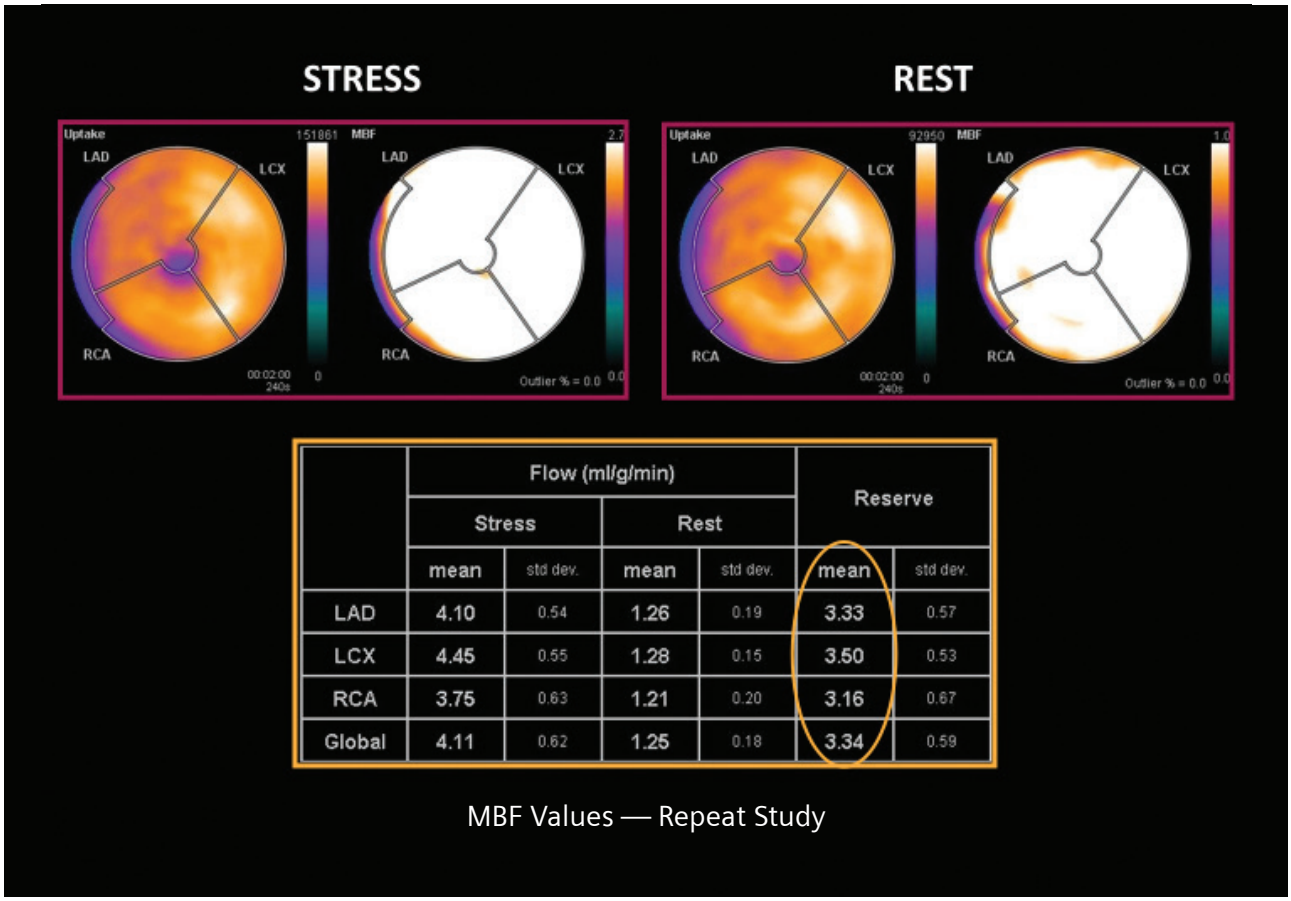

Figure 3: MBF values in the repeat study show an excellent response to adenosine vasodilation, with high MBF at peak stress throughout the entire LV. Both the resting blood flow values and MFR were normal.

in the LAD territory was 4.10 ml/gm/min in the repeat study compared to 1.43 ml/gm/min in the initial study. The mean resting MBF in the LAD territory in the repeat study was 1.26 ml/gm/min, which was remarkably close to the initial study (1.19 ml/gm/min). MFR values in the repeat study were high (global MFR = 3.34), reflecting the increased MBF at peak stress. Compared to the initial study (global MFR = 1.06), the MFR values increased more than 3 times in the repeat study.

The significant increase in values from the initial study's stress MBF to the repeat study's stress MBF, as well as taking into account the remarkable similarity between the two studies' resting MBF tests, suggested that the patient ingested some level of caffeine within 12 hours of the initial study, and that it was likely the cause for the selective decrease in the stress MBF.

Comments

The hyperemic response induced by the adenosine infusion is mediated via stimulation of the A2 membrane adenosine receptors. Theophylline and caffeine are competitive adenosine antagonists and cause decrease in adenosine and dipyridamole mediated vasodilatory response. MBF estimation by dynamic PET is able to quantitatively assess the adequacy of stress response and the effect of caffeine.

In a study by Kubo et al.[1], researchers used O^{15} H_2O PET to evaluate MBF and MFR in 10 healthy volunteers. They used both adenosine and dipyridamole stress, with and without caffeine intake (3 mg/kg of caffeine equivalent to about 2-3 cups of coffee). The resting MBF in both the baseline and caffeine studies did not differ significantly (mean resting MBF = 0.79 ml/gm/min vs. 0.75 ml/gm/min). Without caffeine intake, the mean MBF during adenosine infusion was 3.70 ml/gm/min, and the mean MFR was 5.15. After caffeine intake, the hyperemic flows induced by adenosine were significantly lower (mean resting MBF with caffeine = 1.68 ml/gm/min); there was a corresponding decrease in MFR by more than 40%.

Conclusion

Balanced ischemia is often associated with triple vessel disease because visual evaluation of myocardial perfusion shows uniform uptake throughout the LV, which might be interpreted as normal despite the presence of global ischemia. MBF evaluation, using dynamic PET/CT is a potent tool to identify such balanced ischemia. Low-stress MBF and low MFR in such patients along with associated evidence of transient ischemic dilatation and increased resting ventricular volumes often are important to the diagnosis of advanced CAD. The blunting of stress response with caffeine intake may lead to low-stress MBF with normal resting MBP and may cause a false suspicion of balanced ischemia in at-risk patients. As this clinical case shows, an abnormally low stress MBF in the absence of other evidence of advanced CAD should be interpreted with caution, careful attention should be given to history of caffeine intake and, if required, a repeat study performed with strict adherence to caffeine restriction in order to get to accurate MBF estimations and clinical decision making. ■

Examination Protocol

Scanner: Biograph mCT

SPECT	
Injected Dose	30 mCi (1070 MBq) ^{82}Rb
Scan Delay	Dynamic acquisition triggered by ^{82}Rb infusion
Acquisition	Dynamic list mode; duration, 7 min
CT	Low-dose CT for attenuation correction
Tube Voltage	120 kV
Tube Current	30 mAs
Slice Collimation	3 mm
Slice Thickness	5 mm

References:
[1] Kubo et al. *J Nucl. Med.* 2004; 45: 730–738.

Case 2

^{82}Rb PET/CT Myocardial Blood Flow Estimation for Response Assessment Following Revascularization in Multi-vessel Coronary Artery Disease

By Parthiban Arumugam, MD

Data courtesy of the Department of Nuclear Medicine, Central Manchester University Hospitals, Manchester, United Kingdom

History

A 61-year-old male with a history of dilated cardiomyopathy and left bundle branch block (LBBB) underwent a coronary angiography, which revealed triple vessel disease. The patient was referred for an ^{82}Rb dynamic PET/CT myocardial perfusion study to assess for myocardial ischemia and viability prior to coronary artery bypass grafting (CABG). The study was performed on a Biograph™ mCT scanner.

Following a low-dose CT for attenuation correction, the dynamic ^{82}Rb PET myocardial perfusion study was performed during rest and following adenosine stress. List mode acquisition was started immediately following the start of the IV infusion (30 mCi [1070 MBq] ^{82}Rb). The gated list mode acquisition continued for 7 minutes in both stress and rest studies. Dynamic data was evaluated in *syngo*®.MBF for calculation of myocardial blood flow (MBF). Summed gated stress and rest data were also evaluated in QGS/QPS to visually assess perfusion, and stress and rest left ventricle (LV) function.

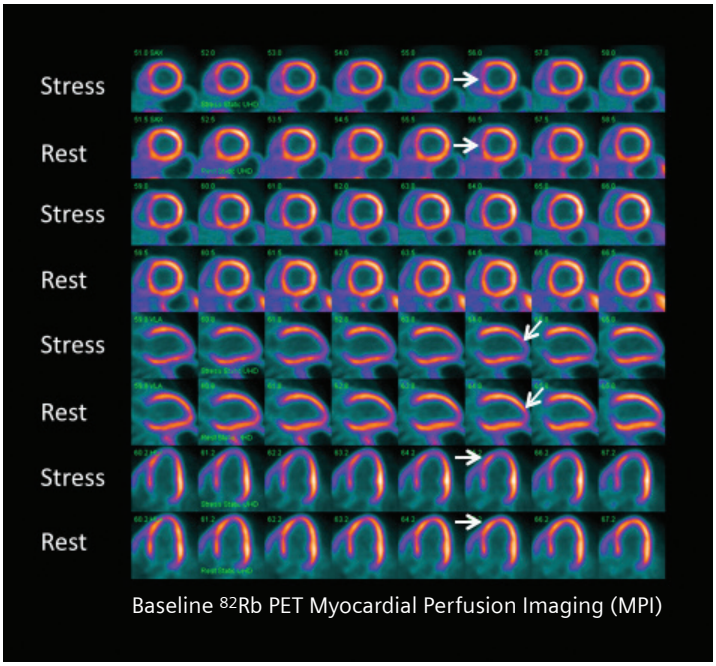

Figure 1: Summed stress and rest images of the baseline ^{82}Rb PET/CT myocardial perfusion study show a dilated LV and a reversible perfusion defect in the septum and apex.

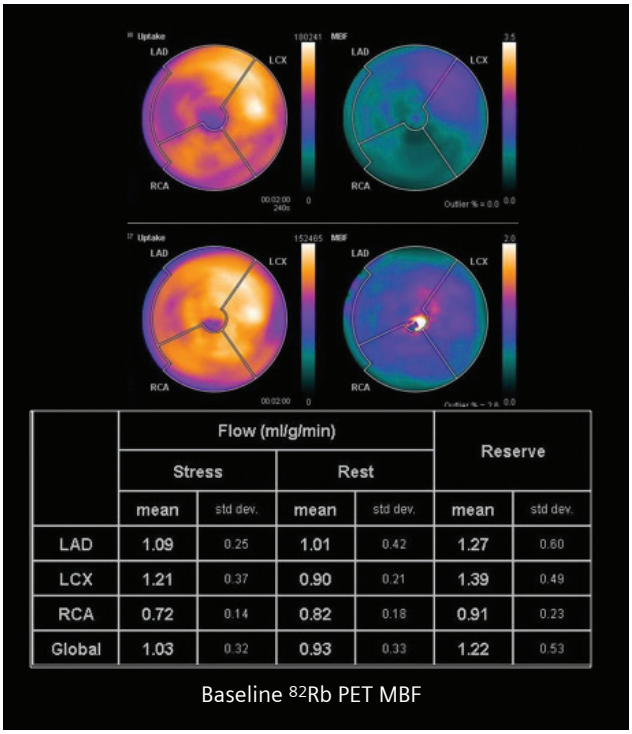

	Flow (ml/g/min)				Reserve	
	Stress		Rest			
	mean	std dev.	mean	std dev.	mean	std dev.
LAD	1.09	0.25	1.01	0.42	1.27	0.60
LCX	1.21	0.37	0.90	0.21	1.39	0.49
RCA	0.72	0.14	0.82	0.18	0.91	0.23
Global	1.03	0.32	0.93	0.33	1.22	0.53

Figure 2: Bulls-eye plot of myocardial uptake and MBF and stress/rest MBF values in ml/gm/min and CFR values show stress inducible ischemia in all arterial territories correlating with triple vessel disease.

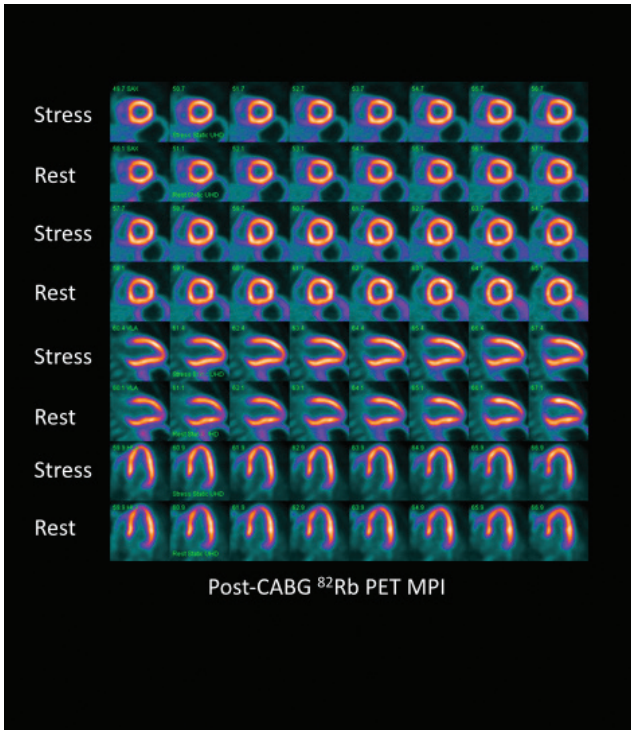

Figure 3: Follow-up stress/rest ^{82}Rb PET myocardial perfusion study shows normal perfusion throughout the entire LV with significant decrease in LV dilatation.

Diagnosis

The baseline ^{82}Rb PET myocardial perfusion study showed a dilated LV and a reversible perfusion abnormality in the apex and septum. The remainder of the LV showed good uptake. The uptake pattern suggested presence of viable myocardium throughout the entire LV.

The rest gated study showed a significantly dilated LV, which had an end diastolic volume (EDV) of 250 ml and an ejection fraction of 17% at rest. There was no significant change in LV volume between stress and rest, reflecting severe ischemic LV dysfunction, secondary to triple vessel disease (ischemic cardiomyopathy).

MBF measurements (*Figure 2*) showed severely impaired MBF throughout the LV involving all 3 arterial territories with significantly compromised myocardial perfusion reserve. Mean peak-stress blood flow in the left anterior descending (LAD) territory was 1.09 ml/gm/min, while the lower range for normal is around 2.5 ml/gm/min. The septum showed mild inducible ischemia on the visual evaluation of stress/rest images and bulls-eye plot. However, the MBF and coronary flow reserve (CFR) values demonstrated severe global left ventricular myocardial ischemia. The resting blood flow values were within normal limits, with significantly restricted CFR values, suggesting severe ischemic, but viable myocardium. CFR in the right coronary artery (RCA) territory was 0.91, while the normal is above 2.

Based on the PET/CT evaluation, which suggested severe global LV ischemia with completely viable myocardium that correlated with angiographic findings of triple vessel disease, the patient was advised CABG. The patient successfully underwent a successful three-vessel CABG the month after the initial PET/CT study.

Two months following CABG, the patient presented again with increasing dyspnoea and atypical chest pain. There was, however, no troponin rise, which suggested an absence of acute myocardial infarction or myocyte injury. Because of the symptoms, the patient was sent for a repeat ^{82}Rb stress/rest PET/CT myocardial perfusion study.

The follow-up dynamic ^{82}Rb PET/CT study, which was performed using a protocol similar to the baseline study, showed normal perfusion throughout the entire LV. There was significant decrease in LV cavity dilatation. LV function had improved considerably

with an ejection fraction of 43% and LV diastolic volume of 136 ml.

MBF also showed significant improvement (*Figure 4*) with normalization of stress MBF in all arterial territories. The resting flow values also showed a slight increase in comparison to the baseline study. CFR values showed significant increase compared to the baseline study. CFR in RCA territory increased from 0.91 in the baseline study to 2.18 in the post-CABG study, suggesting that the peak stress MBF more than doubled following CABG.

Resting left ventricular ejection fraction (LVEF) increased from 17% to 43% following CABG, which reflected the severe ischemic ventricular dysfunction caused by multivessel disease and the preserved viability identified by the myocardial perfusion study that led to such dramatic improvement following revascularization.

Comments

This study highlights the value of stress/rest MBF measurements with dynamic PET/CT in delineating the true extent of myocardial ischemia, especially in patients with balanced ischemia secondary to triple vessel disease.

In this patient, visual evaluation of baseline stress/rest PET myocardial perfusion demonstrated inducible ischemia only in the septum and apex. The only visual evidence of advanced CAD was the LV dilatation, which was severe even at rest and had the low resting LVEF of 17%. Due to the severity of LV dilatation at rest and resting ventricular dysfunction, further stress-induced LV dysfunction was not visually apparent. Only with MBF estimation was the severe global reduction in MBF at peak stress involving all 3 arterial territories apparent. The resting MBF values were within the normal range. However, the resting LV dilatation and low resting LVEF, in spite of resting blood flow within normal range, was typical of hibernating myocardium.

Hibernating myocardium is associated with a decrease in wall motion during rest. This helps to preserve myocyte function as well as compensate for lower levels of resting flow and for compromised MBF increases that occur with increased myocardial workloads. Hibernating myocardium is also associated with preserved myocardial viability, as is demonstrated in this clinical case by the adequate resting perfusion, ^{82}Rb uptake and resting MBF all within normal limits. Usually, hibernating myocardium can recover significantly following revascularization, including resting wall motion and LVEF. As well, an improvement in stress response can often occur. This was clearly demonstrated in the improvement in stress MBF in the post-CABG study with increases of more than 100% in some myocardial segments. The resting blood flow was also slightly improved

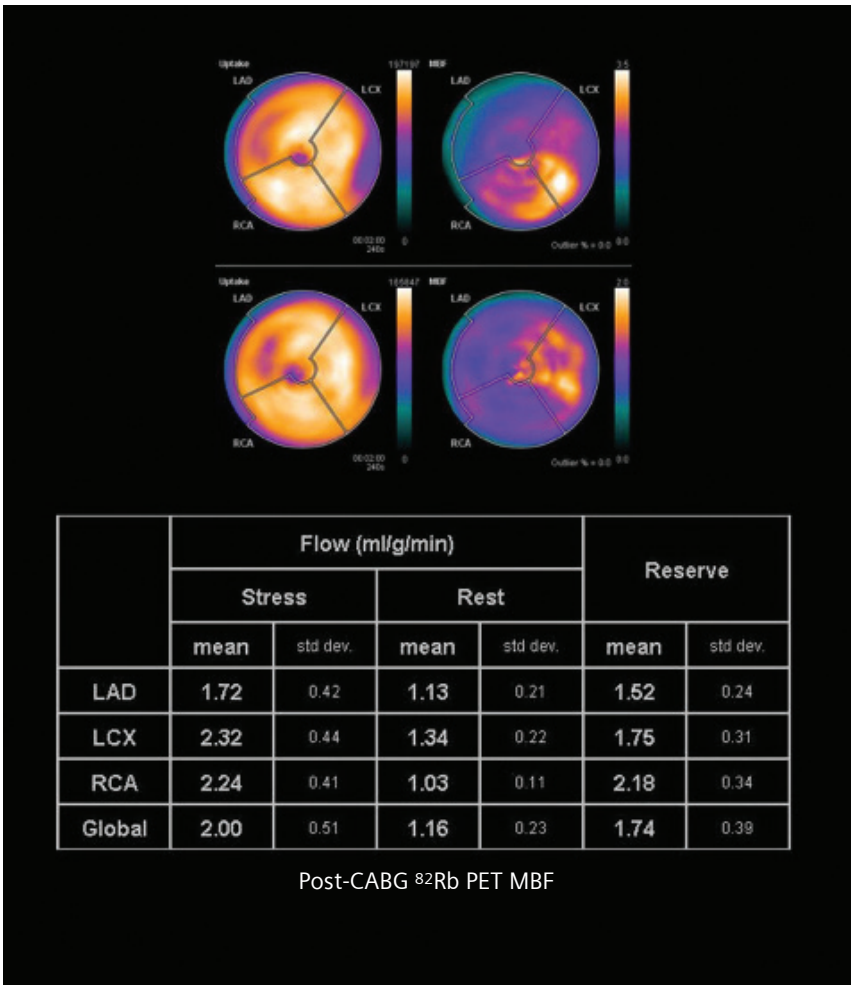

	Flow (ml/g/min)				Reserve	
	Stress		Rest			
	mean	std dev.	mean	std dev.	mean	std dev.
LAD	1.72	0.42	1.13	0.21	1.52	0.24
LCX	2.32	0.44	1.34	0.22	1.75	0.31
RCA	2.24	0.41	1.03	0.11	2.18	0.34
Global	2.00	0.51	1.16	0.23	1.74	0.39

Post-CABG ^{82}Rb PET MBF

Figure 4: Post-CABG dynamic PET perfusion study shows normal myocardial uptake, and global and regional stress MBF.

following revascularization, suggesting that baseline resting blood flow was compromised by the severe triple-vessel stenosis, reflected by resting LV dysfunction.

In dysfunctional myocardial segments related to severe stenosis, resting MBF has shown to vary from normal to reduced. In a study[1] involving 116 patients with ischemic cardiomyopathy, 46% of all myocardial segments were dysfunctional. 72% of these dysfunctional segments showed normal resting MBF (>0.6 ml/gm/min). Dysfunctional myocardial segments with normal resting MBF and preserved, or reduced, glucose metabolism were interpreted as chronic stunning. 9% of the segments showed reduced resting MBF (<0.6 ml/gm/min) and preserved glucose uptake and were interpreted as hibernating myocardium.

Revascularization in patients with ischemic LV dysfunction with preserved viability is usually associated with early improvement in LVEF. In a recent study[2], mean resting LVEF increased from 18% to 30% within 1 month after revascularization in patients with ischemic LV dysfunction and multi-vessel disease.

Conclusion

In the present study, the improvement in stress and resting MBF, as well as the resting LVEF following revascularization, reflects the clinical value of dynamic ^{82}Rb PET myocardial perfusion. It provides both visual and quantitative assessments of ischemia, as well as a ventricular functional evaluation in a single study that can accurately determine the response to pharmacological stress—all of which help the processes of clinical decision making and revascularization follow-up. ■

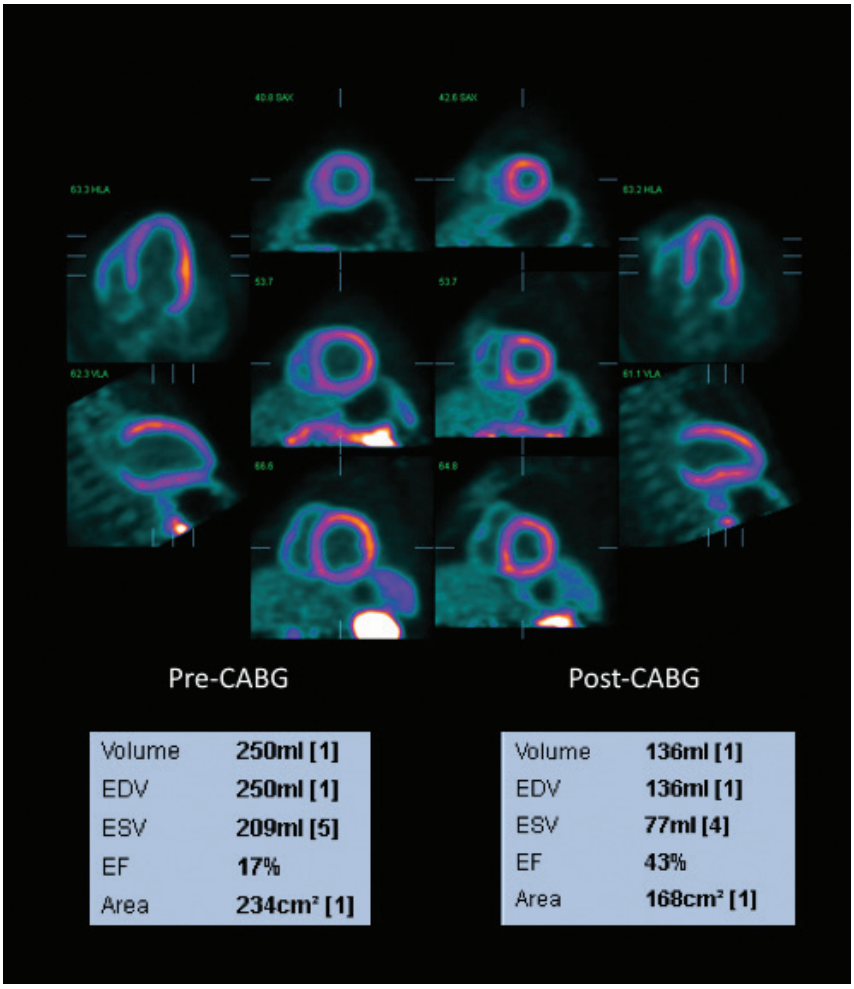

Figure 5: Comparison of different cross sectional views of myocardial perfusion and LV functional indexes like EDV and LVEF before and after CABG shows the improvement in LV function following revascularization.

Examination Protocol

Scanner: Biograph mCT

PET	
Injected Dose	30 mCi (1070 MBq) ^{82}Rb
Scan Delay	Dynamic acquisition triggered by ^{82}Rb infusion
Acquisition	Dynamic list mode; duration, 7 min
CT	Low-dose CT for attenuation correction
Tube Voltage	120 kV
Tube Current	30 mAs
Slice Collimation	3 mm
Slice Thickness	5 mm

References:
[1] Hernandez-Pampaloni et al. *Eur J Nucl Med Mol Imaging.* 2005. 32: 314–321.
[2] *Med Arch.* 2014, Oct. 68(5): 332-334.

Case 3

Myocardial Viability Assessment with ^{18}F FDG* PET/CT Study in a Case of Ischemic Cardiomyopathy

By Jean Gregoire, MD, Department Head, Nuclear Medicine

Data courtesy of Montreal Institute of Cardiology, Montreal, Canada

History
A 67-year-old male, who smokes and has a history of type-II diabetes and dyslipidemia, presented with progressive shortness of breath over 3 weeks. Additionally, the patient showed development of pedal edema over 2 days. The dyspnea and fatigue were severe enough to limit daily activities. The patient had no known history of coronary artery disease (CAD) and had never complained of chest pain. The progression of dyspnea was significant, since the patient had progressed from AHA functional class I to class III in 3 weeks. As such, the clinical impression was bilateral heart failure with progressive pulmonary edema. Serum troponin was negative, which suggested an absence of acute myocardial injury or an infarction. The patient was initially evaluated with echocardiography.

The echocardiography revealed a dilated left ventricle (LV) with an apical thrombus (*Figure 1*). There was an akinesis of the anterior wall, the septum wall and the antero-apical segment. The left ventricle ejection fraction (LVEF) was 15%. There was also mild tricuspid regurgitation. Right ventricular (RV) systolic dysfunction reflected pulmonary hypertension.

The patient developed progressive pulmonary edema leading to cardiogenic shock, and he also had asymptomatic episodes of ventricular tachycardia. Therefore, the patient was admitted to Montreal Institute of Cardiology in Montreal, Canada, where he was initially stabilized with an intra-aortic balloon. Subsequently, the patient underwent coronary angiography.

Coronary angiography (*Figure 2*) showed 100% ostial stenosis of the left anterior descending (LAD) and 100% stenosis in the proximal right coronary artery (RCA). There was 50% stenosis of the mid-left circumflex (LCX) and the

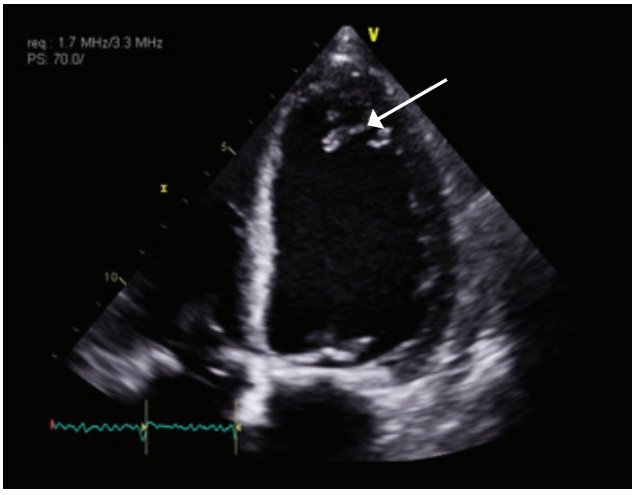

Figure 1: Apical 4-chamber view of the echocardiogram shows dilated LV with apical thrombus (*arrow*).

left marginal artery. A ventriculogram revealed severe diffuse hypokinesia with a LVEF of 10-15%.

With severe LAD and RCA stenosis and the gross hypokinesia of the anteroseptal wall, the decision to perform revascularization required confirmation of the presence of viable myocardium in the affected arterial territories. An MRI viability study was performed.

Non-contrast morphological MR images including breathe-hold HASTE and TrueFISP Cine showed a dilated LV with severe diffuse hypokinesia and decreased LVEF of 17%. The right ventricle ejection fraction (RVEF) was 27%. The anterior wall, septum and apex appeared thinned with severe hypokinesia.

Post-contrast MR images showed transmural contrast enhancement in the whole of septum, anterior wall, apex and adjacent anteroapical segment. Lateral and inferolateral walls showed an absence of gandolium (Gd) enhancement. The study suggested an absence of viability in the LAD territory, while RCA and LCX territories—inferior, inferolateral and posterolateral walls—showed viable myocardium.

With an absence of viability in the entire LAD territory, along with severe hypokinesia of the anterior wall and septum, and a low resting LVEF, revascularization was not considered an option. The patient was referred for a heart transplant evaluation. However, during further review in the medico-surgery meeting, it was suggested that F 18 Fludeoxyglucose (^{18}F FDG) PET/CT for myocardial viability assessment be performed in order to confirm an absence of any LAD territory myocardial viability prior to eliminating revascularization as a therapy option.

The patient underwent ^{18}F FDG PET/CT using a standard protocol with glucose loading along with intravenous insulin. The patient was injected with 8 mCi (296 MBq) of ^{18}F FDG intravenously. The patient also received rapid intravenous injection of 9 units of insulin. The blood glucose level at the time of injection was 7.2 mmol/L. 62 minutes post-injection, following a low-dose CT for attenuation correction, gated list mode PET acquisition was performed for 10 minutes.

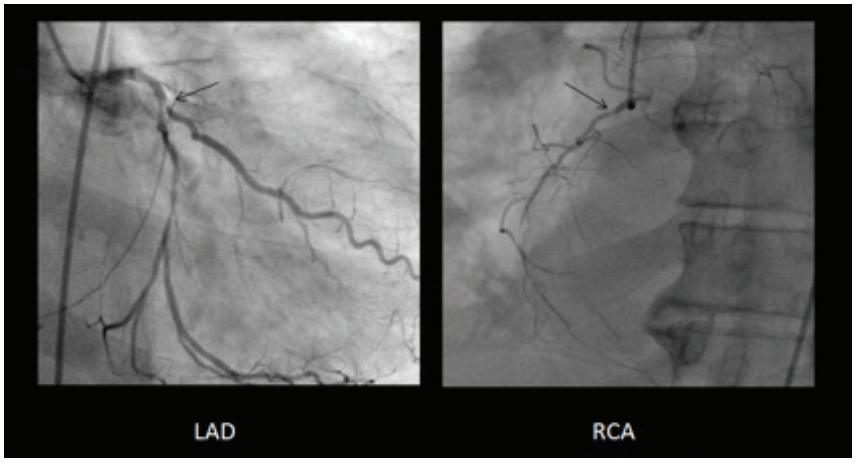

Figure 2: Coronary angiography shows proximal LAD and RCA stenosis.

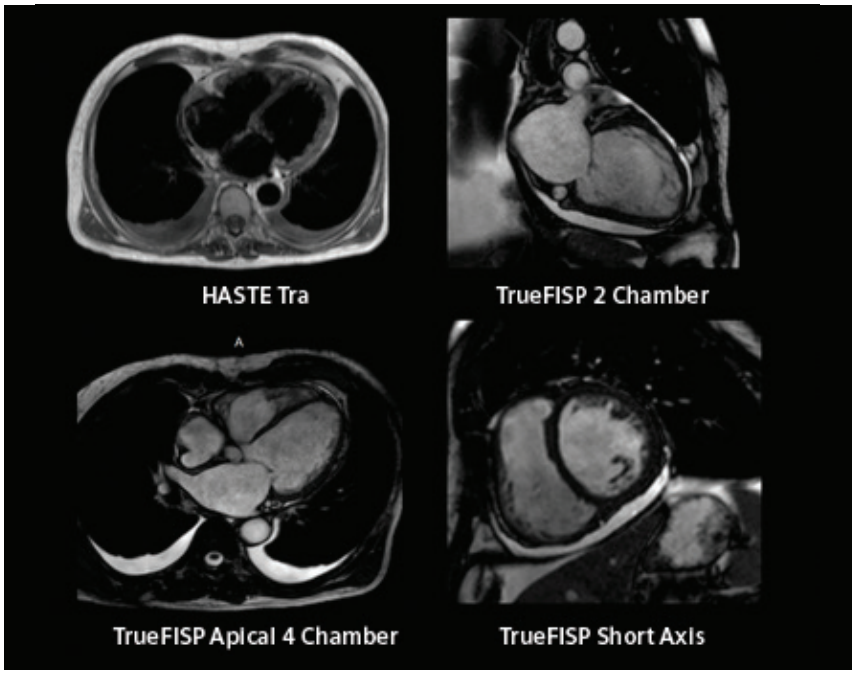

Figure 3: Non-contrast MR images show a dilated LV with thinning of the anterior wall, septum and apex.

Diagnosis

^{18}F FDG PET/CT viability images showed a thinned myocardium with slightly lower than normal, but well-preserved tracer uptake in the septum, apex, anterior wall and anteroapical segment. The lateral, inferolateral and posterolateral wall showed normal tracer uptake with preserved myocardial thickness. The LV cavity showed gross dilatation with severe diffuse hypokinesia with LVEF of 20%.

The PET/CT viability study clearly showed significant ^{18}F FDG uptake in the myocardium involving the whole of the LAD territory, which suggested preserved viability of the entire arterial territory. Since the RCA and LCX territories also showed preserved ^{18}F FDG uptake, the PET/CT study suggested complete reversibility of the entire LV. This was in stark contrast to the MRI findings that demonstrated delayed contrast enhancement in the septum, apex and anterior wall and suggested absence of LAD territory viability. In view of the PET/CT findings, the patient underwent coronary artery bypass grafting (CABG).

The patient had a slow recovery following CABG. Upon discharge his echocardiography showed significant improvement in LVEF, which increased to 30%, while pre-CABG LVEF was 15%. The patient had one follow-up visit and showed significant improvement in physical capacity (AHA functional class I). Early improvement in cardiovascular function following CABG further confirmed the PET/CT findings of viability in the LAD territory, which showed improved contractility leading to LVEF following CABG.

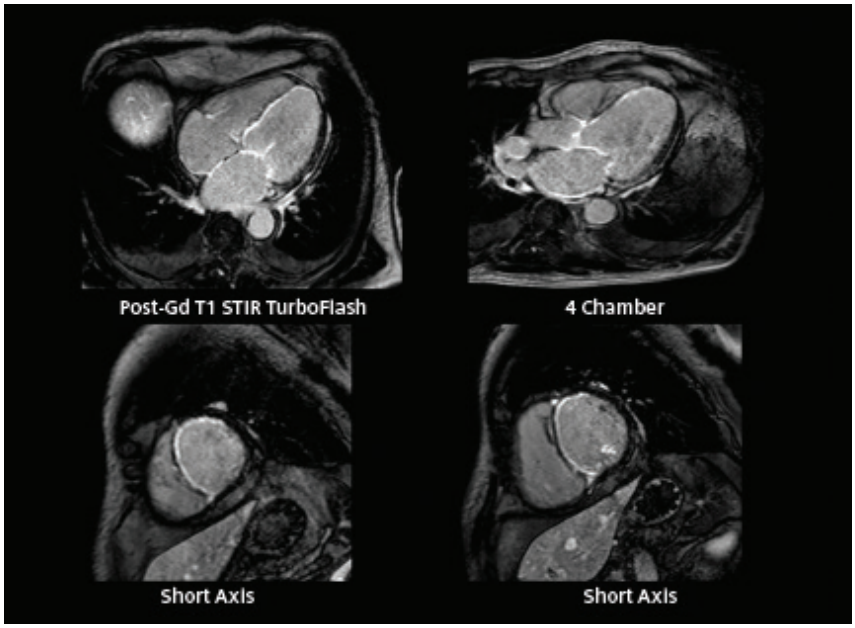

Figure 4: Post-Gd T1 fat suppressed images show contrast enhancement in the whole of septum, anterior wall and apex.

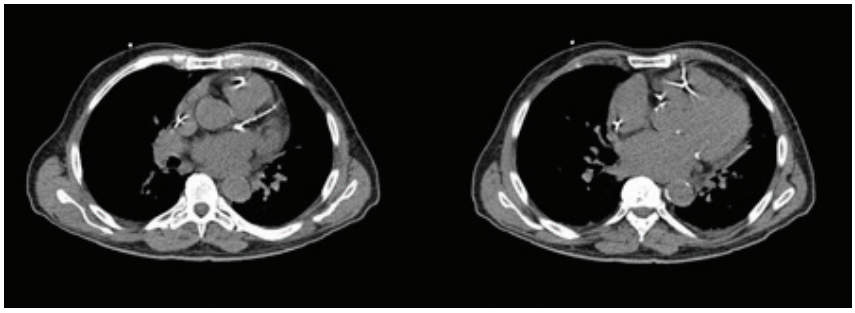

Figure 5: Non-contrast CT images show severe calcification throughout the LAD and multiple focal calcifications in the RCA and LCX.

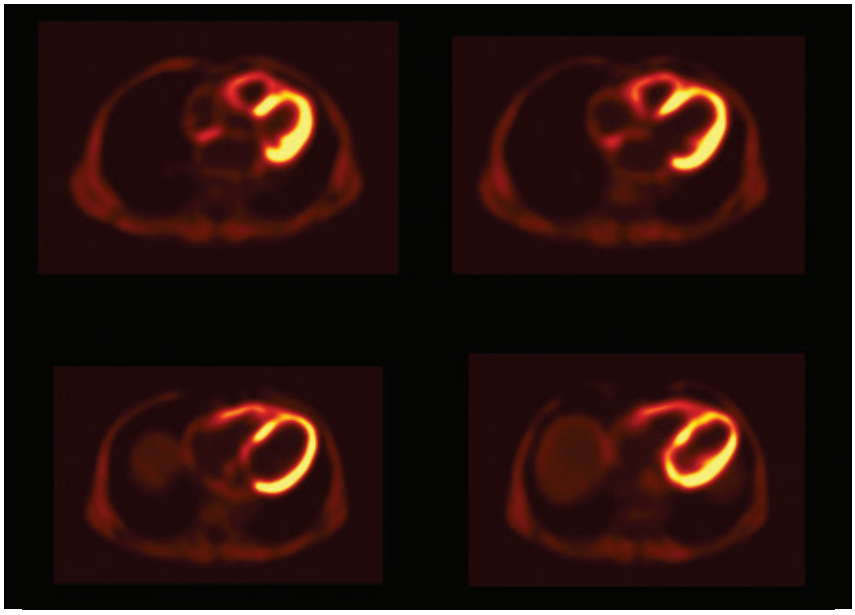

Figure 6: Summed-^{18}F-FDG-PET-axial images show slightly lower, but preserved ^{18}F FDG uptake in the septum and anterior wall.

Comments

This case study highlighted divergence in viability estimation between ^{18}F FDG PET/CT and contrast MRI. The intensity of ^{18}F FDG uptake visualized on PET/CT suggested the presence of viable myocardium in the entire LAD territory, while the same myocardial segments showed delayed enhancement of Gd contrast on MRI, which reflected absence of viability within the infarcted segments. However, post-CABG, the overall improvement in myocardial contractility and LVEF all suggested significant recovery of contractility in the LAD territory. This confirms the PET/CT finding of preserved viability in the LAD territory since functional improvement following CABG would not be possible without significant recovery of anteroseptal contractility.

Discrepancy between ^{18}F FDG PET/CT and delayed enhancement on contrast MRI for assessment of myocardial viability has been demonstrated in several studies. Hunold et al.[1] compared Gd MRI and ^{18}F FDG PET/CT findings in a total of 1753 myocardial segments in patients with advanced CAD. In MRI, 40% of the segments showed myocardial scar, whereas PET/CT revealed impaired uptake in 25%. Using PET/CT as the standard of reference, contrast-enhanced MRI had a specificity of 76% for the detection of scars. 18% of all segments showed late Gd enhancement, but normal ^{18}F FDG uptake. 83% of these segments were classified as sub-endocardial scars.

In another study, delayed enhancement with Gd MRI was classified according to the extent of transmural enhancement; enhancement >50% of myocardial thickness was taken as the cutoff for estimation of non-viability.[2] Absence of ^{18}F FDG uptake correlated strongly with an absence of recovery following CABG, while the cutoff of >50% enhancement of the myocardial thickness correlated poorly with functional recovery. While an absence of delayed enhancement was highly predictive of functional recovery following revascularization, delayed enhancement (>50%) showed a specificity of 44%, reflecting the presence of segments with sub-endocardial infarction that were visually

classified as >50% thickness enhancement and wrongly labelled as non-viable. ^{18}F FDG PET/CT, on the other hand, was highly specific (98.8%), and the absence of ^{18}F FDG uptake correlated highly with the absence of functional recovery.

Conclusion

Delayed enhancement on contrast MRI represents irreversible myocardial injury. However, the amount of viable myocardium within a segment with contrast enhancement varies depending on the sub-endocardial or transmural nature of the enhancement. The discrepancy between MRI findings of transmural Gd enhancement and adequate myocardial uptake of ^{18}F FDG on PET/CT in this patient may be secondary to presence of predominantly sub-endocardial myocardial injury secondary to long standing severe resting ischemia and repeated myocardial stunning. ^{18}F FDG PET/CT, though, reflects uptake in viable myocytes with intact membranes and, thus, may be a more sensitive indicator of viable myocardium and recovery following revascularization. ■

Examination Protocol

Scanner: Biograph mCT 128

PET	
Injected Dose	8 mCi (296 MBq) ^{18}F FDG
Scan Delay	62 min
Acquisition	Gated list mode
CT	Low-dose CTAC
Tube Voltage	120 kV
Tube Current	40 mAs
Slice Collimation	2.5 mm
Slice Thickness	3 mm

References:
[1] Hunold et al. Rofo. 2002 Jul; 174(7): 867-873.
[2] Wu et al. *J Nucl Med* 2007; 48:1096–1103.

* The full prescribing information can be found on pages 42-44.

The statements by Siemens customers described herein are based on results that were achieved in the customer's unique setting. Since there is no "typical" hospital and many variables exists (e.g., hospital size, case mix, level of IT adoption) there can be no guarantee that other customers will achieve the same results.

Case 4

Detection of Graft Blockage by ^{82}Rb PET/CT Myocardial Blood Flow Estimation

By Nimish Dhruva, MD

Data courtesy of Piedmont Heart, Atlanta, GA, USA

History
A 65-year-old, obese male with a history of coronary artery disease (CAD) that was treated with coronary artery bypass grafting (CABG) 5 years back, presented with gradually progressive chest pain and breathlessness. As such, the patient underwent SPECT myocardial perfusion scintigraphy using pharmacological stress with regadenoson. It was reported as normal. However, the patient continued to have chest pain despite continued drug therapy. Therefore, the patient was referred for an ^{82}Rb PET/CT myocardial perfusion study.

The study was performed on a Biograph™ mCT. Dynamic list mode acquisition was started immediately following an infusion of ^{82}Rb (40 mCi [1040 MBq]) during regadenoson stress. Dynamic stress acquisition continued for 7 minutes. Using an identical protocol, rest acquisition was performed soon after the stress study. List mode data was processed by *syngo*®.MBF to evaluate myocardial blood flow (MBF) values during stress and rest.

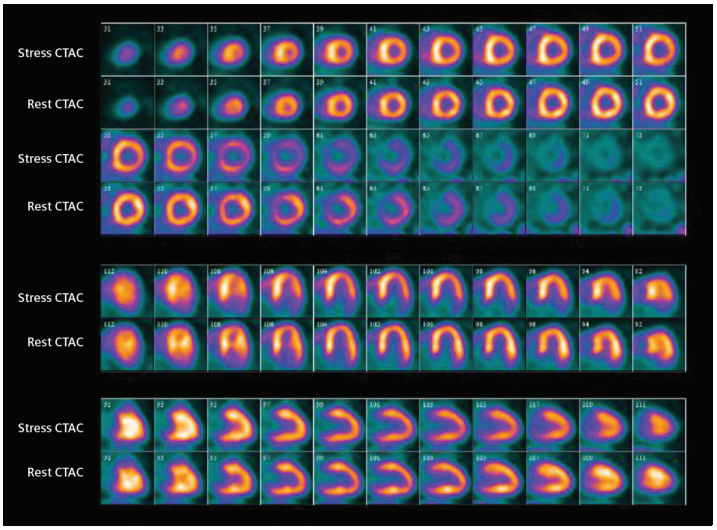

Figure 1: Stress/rest ^{82}Rb PET/CT myocardial perfusion study shows reversible ischemia in the posterolateral wall.

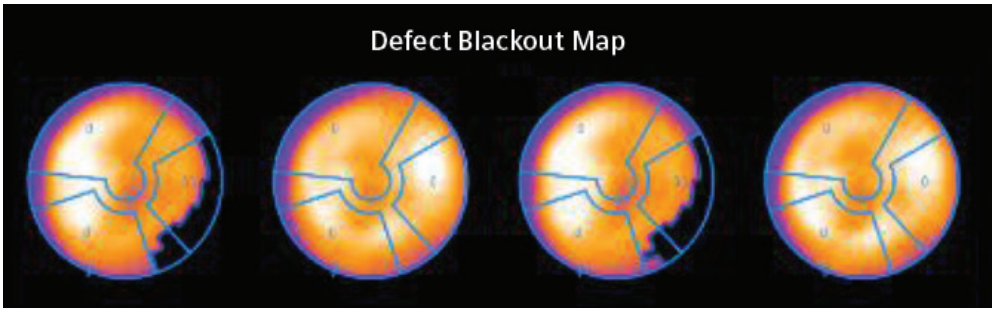

Figure 2: Bulls-eye plot and defect blackout map show reversible ischemia in the posterolateral and posterobasal region that correlates with the LCX territory ischemia.

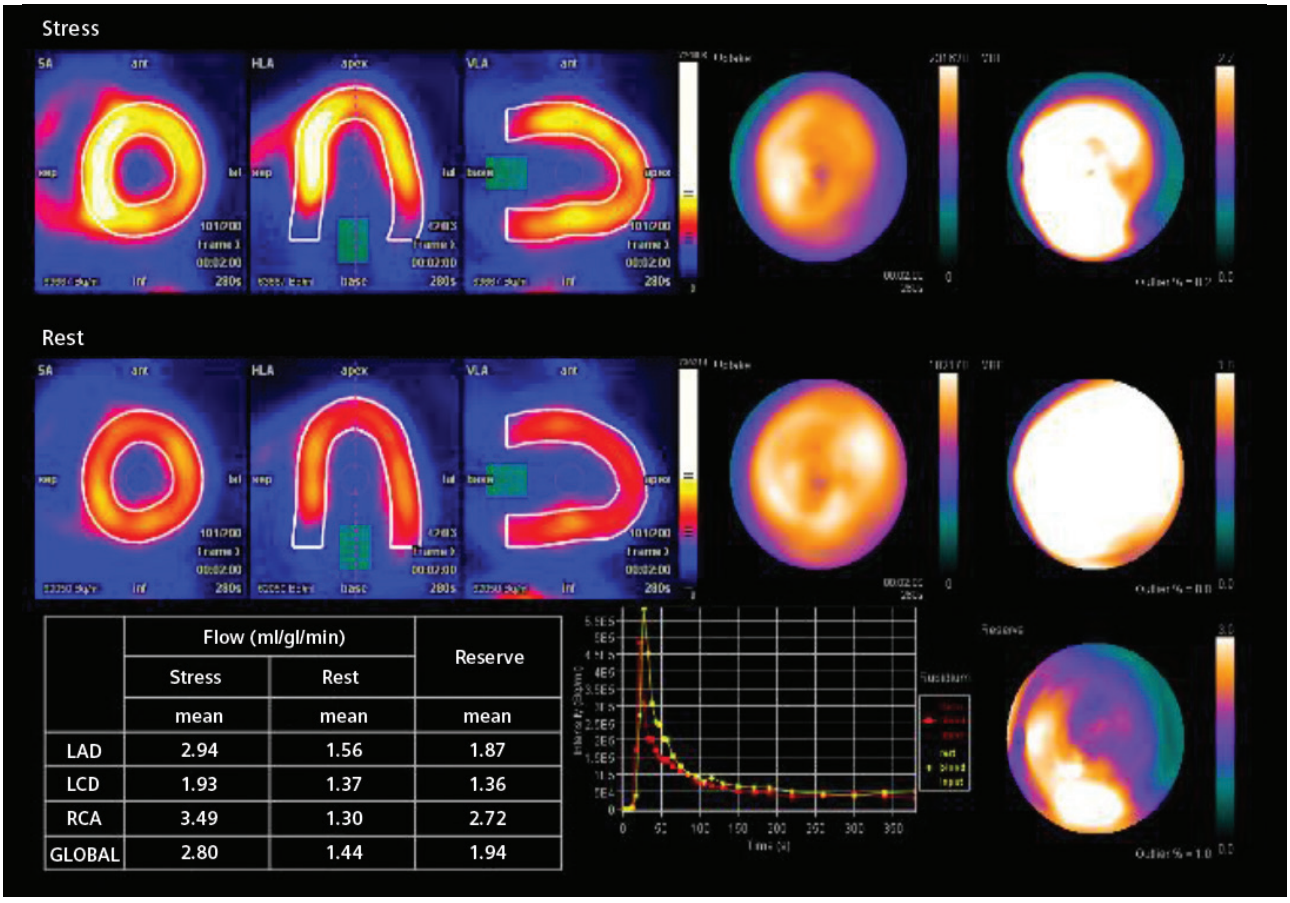

	Flow (ml/gl/min)		Reserve
	Stress	Rest	
	mean	mean	mean
LAD	2.94	1.56	1.87
LCD	1.93	1.37	1.36
RCA	3.49	1.30	2.72
GLOBAL	2.80	1.44	1.94

Figure 3: MBF estimation on *syngo*.MBF shows decreased stress flow in the LCX region.

Diagnosis

Summed stress and rest images (*Figure 1*) showed a reversible perfusion defect in the posterolateral wall. The anterior, inferior and septum walls demonstrated normal tracer uptake. The left ventricle (LV) appeared normal in size, with mild post-stress dilatation. The study was consistent with reversible ischemia in the left circumflex (LCX) territory.

MBF estimation (*Figure 3*) showed decreased flow during stress in the LCX region, while the stress flow is normal in the left anterior descending (LAD) and right coronary artery (RCA) territories. The mean MBF in the LCX region was 1.93 ml/gm/min and was 2.94 ml/gm/min for the LAD. Compared to the LAD territory, the LCX flow values were significantly lower and correlated with the visual evaluation of reversible perfusion defect.

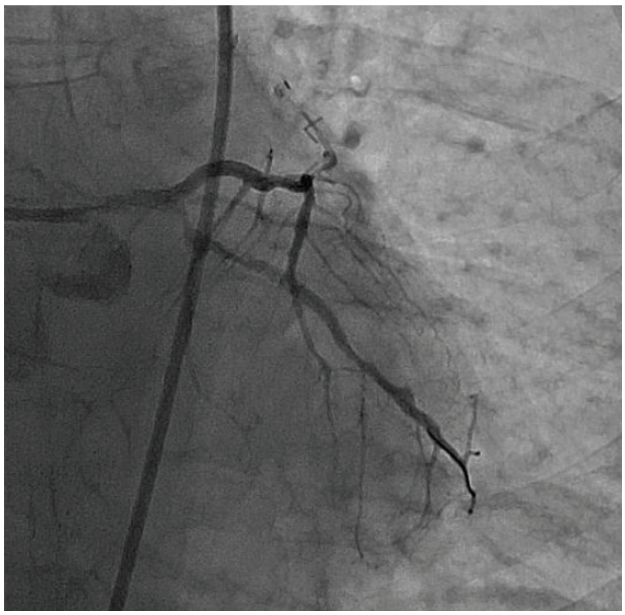

Figure 4: Coronary angiography shows blockage of venous graft to LCX along with tight proximity to the LM and ostial circumflex stenosis.

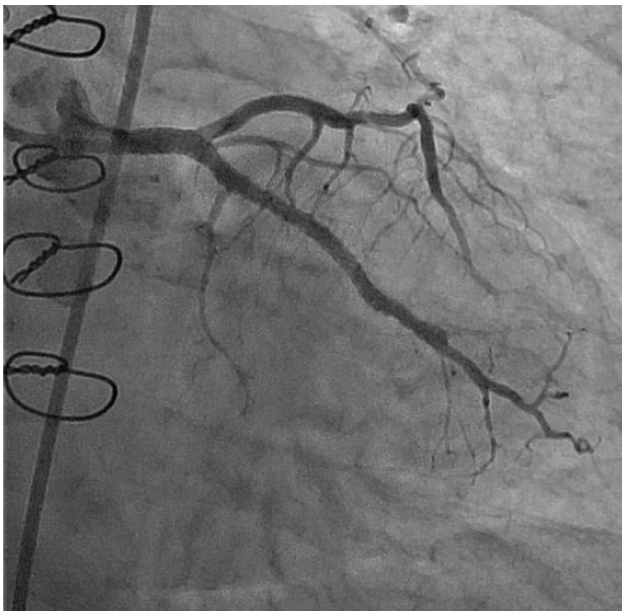

Figure 5: Post-revascularization coronary angiography shows improved blood flow in the LCX and in the LAD.

Myocardial flow reserve in the LCX territory was 1.38 ml/gm/min while the normal average is around 2 to 2.5 ml/gm/min. The absolute blood flow value in the LCX territory (1.93 ml/gm/min) was, however, only borderline below the lower limit of normal, thus suggesting mild to moderate ischemia. Resting MBF values in all arterial territories were similar.

In view of the PET/CT evaluation that suggested inducible ischemia in the LCX territory, the patient was subjected to a coronary angiography.

Comments
This study demonstrated the high sensitivity and accuracy of PET/CT myocardial perfusion for evaluation of inducible ischemia. Although the initial SPECT study was reported as normal, using the same stress agent (regadenoson) in the PET/CT evaluation showed reversible ischemia in the LCX region. This may reflect the improved image quality achieved with PET/CT and a more robust attenuation correction, as well as the assessment of ventricular response to pharmacological stress immediately following infusion of the stress agent. MBF evaluation is also helpful when evaluating early ischemia, as in this case where the MBF values were lower in the LCX territories compared to that of RCA or LAD. Coronary angiography was consistent with the PET findings.

Conclusion
MBF quantification with PET/CT is able to delineate limited ischemia, secondary to coronary bypass graft blockage, in a patient for whom SPECT perfusion was normal due to improved image quality, robust attenuation correction and absolute quantification capabilities. ■

Examination Protocol

Scanner: Biograph mCT

PET	
Injected Dose	40 mCi (1040 MBq) ^{82}Rb
Scan Delay	Immediate acquisition
Acquisition	Dynamic list mode (stress/rest)
CT	
Tube Voltage	120 kV
Tube Current	30 mAs
Slice Collimation	3 mm
Slice Thickness	5 mm

The statements by Siemens' customers described herein are based on results that were achieved in the customer's unique setting. Since there is no "typical" hospital and many variables exist (e.g., hospital size, case mix level of IT adoption) there can be no guarantee that other customers will achieve the same results.

Case 5

Delineation of Multi-vessel Coronary Artery Disease with ^{82}Rb PET/CT Myocardial Perfusion and Blood Flow Estimation

By Nimish Dhruva, MD

Data courtesy of Piedmont Heart, Atlanta, GA, USA

History
A 68-year-old male, who has a long-standing history of diabetes, presented with progressively increasing shortness of breath during exertion. Suspicious for coronary artery disease (CAD), the patient underwent an ^{82}Rb PET/CT myocardial perfusion study with regadenoson during stress and rest. The study was performed on a Biograph™ mCT.

Immediately following an infusion of ^{82}Rb (40 mCi [1480 MBq]) during regadenoson stress, the dynamic list mode acquisition began. Dynamic stress acquisition continued for 7 minutes. Soon after, a rest acquisition was performed using a protocol identical to that used during stress. The list mode data was processed by *syngo*®.MBF for evaluation of myocardial blood flow (MBF) values during stress and rest.

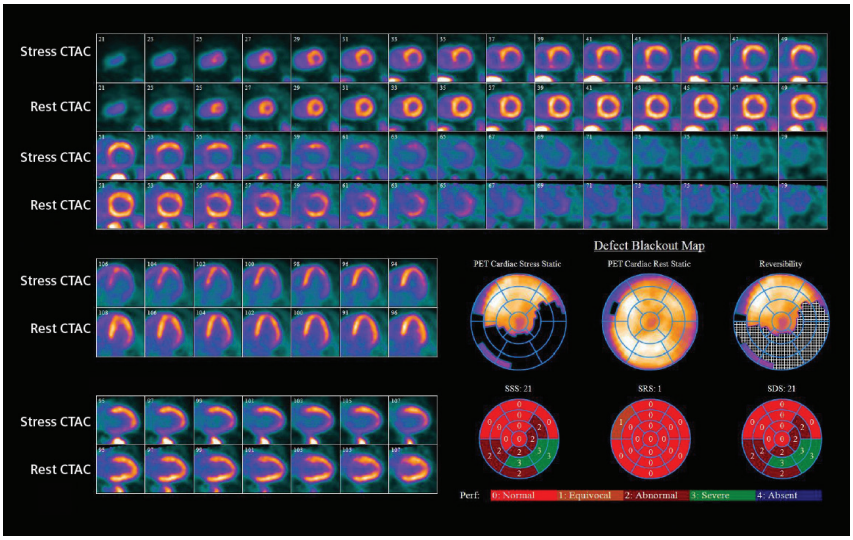

Figure 1: ^{82}Rb PET myocardial perfusion study shows a severe perfusion defect in the inferior, inferolateral and lateral walls, with complete reversibility.

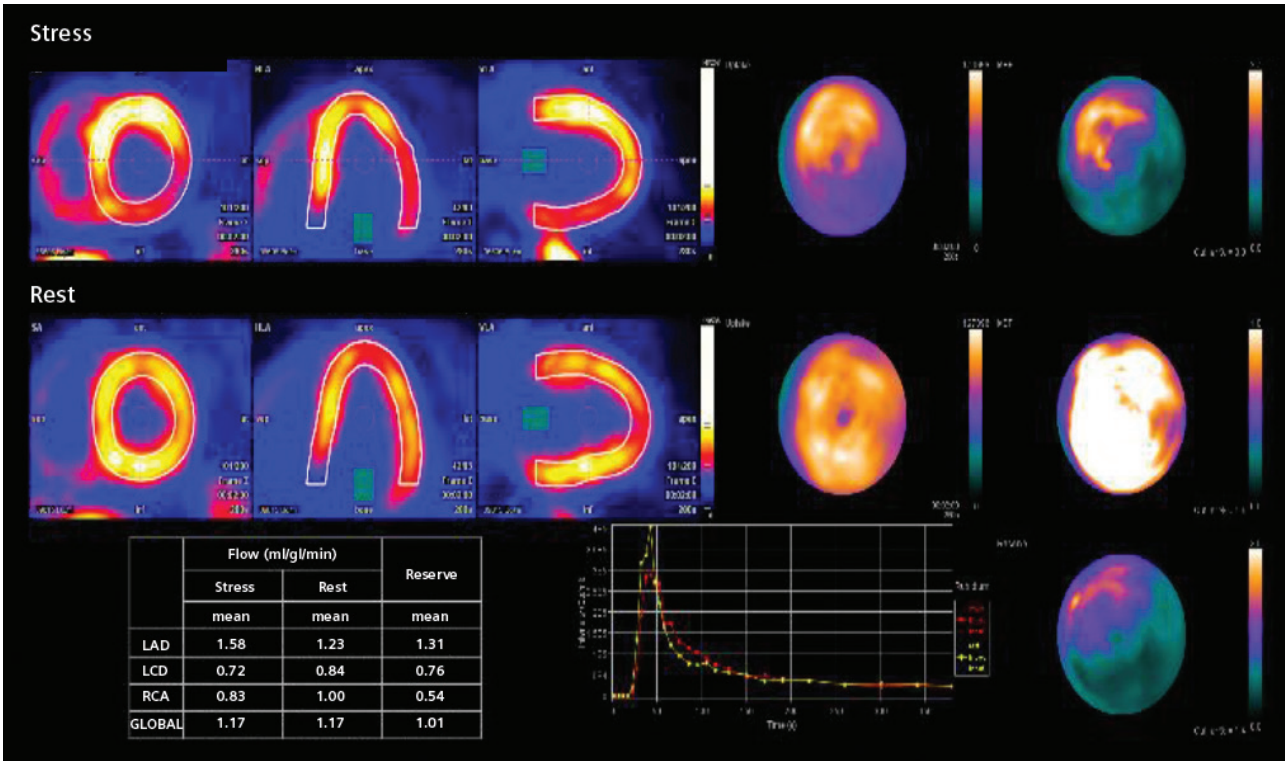

Figure 2: MBF estimation shows low-stress MBF values in all arterial territories, with the lowest value in LCX and RCA territories, as well as a low myocardial flow reserve.

Diagnosis

The ^{82}Rb PET/CT myocardial perfusion study showed severe ischemia in the inferior, inferolateral and lateral walls, with complete reversibility of the entire ischemic area, demonstrated by the normal uptake at rest. There was significant post-stress left ventricular (LV) dilatation (transient ischemic dilatation), which reflected advanced and, possibly, multi-vessel disease. The pattern of the ischemia suggested severe stenosis in the right coronary artery (RCA) and left circumflex (LCX). The resting LV ejection fraction (LVEF) was 43%. The LVEF at peak stress was 48%.

MBF, estimated by *syngo*.MBF, showed decreased stress MBF in all arterial territories, with severely decreased stress flow values in the RCA and LCX territories. The mean MBF in the RCA territory was 0.83 ml/gm/min. (The normal range at peak stress is 2-2.5 ml/gm/min.) The LCX territory showed a severely reduced mean stress MBF of 0.73 ml/gm/min. Although, visually, the anterior wall and septum (left anterior descending [LAD] territory) showed normal tracer uptake, the stress MBF in LAD territory was also significantly reduced (1.52 ml/gm/min).

Resting MBF values for all arterial territories were similar and within normal limits. However, the resting MBF of the LCX territory (0.86 ml/gm/min) was substantially lower compared to the resting MBF values of the left ventricle myocardium. The resting MBF values in the RCA and LCX territories were slightly higher than the MBF values at peak stress, which suggested severe stenosis. Myocardial flow reserve was low for all arterial segments, particularly for the LCX and RCA territories (0.76 and 0.54), but was also low for the LAD territory (1.34). With normal flow reserve

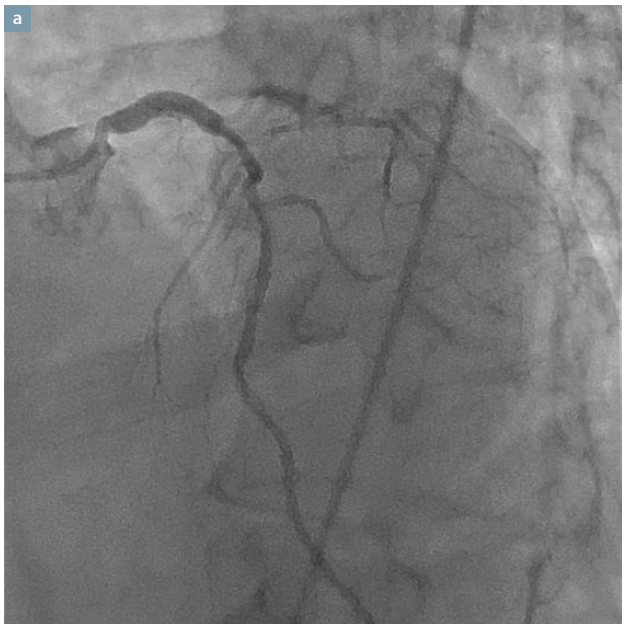

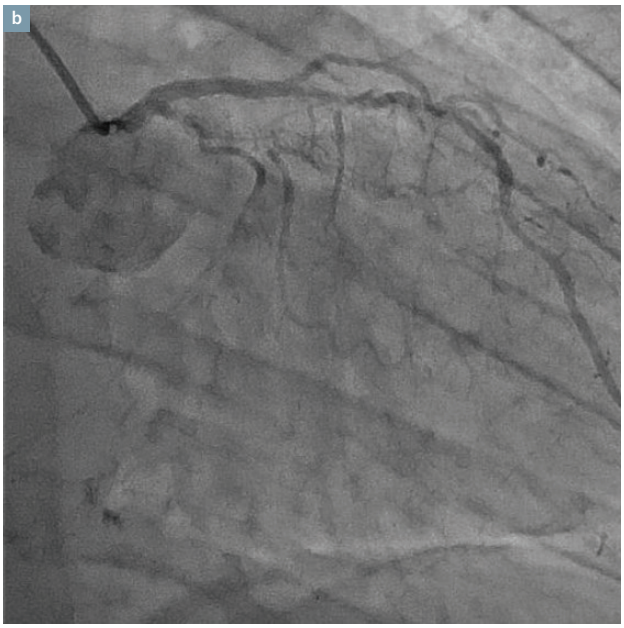

Figure 3 (a-c): Coronary angiography shows moderate stenosis in the proximal LAD (a), tight proximal LCX stenosis (b) and severe stenosis of the mid-right coronary artery (c).

values expected to be >2.5, severe inducible ischemia in RCA and LCX territories and moderate ischemia in the LAD territory was expected.

The pattern of perfusion defects in the ^{82}Rb PET/CT study and the MBF and flow reserve estimates suggested triple vessel disease, with the most severe stenosis in the RCA and LCX. The patient underwent coronary angiography.

Coronary angiography showed tight stenosis in the mid-RCA and proximal LCX. The proximal and mid-LAD also showed moderate diffuse stenosis. Because of both the PET impression and angiography findings, the patient was advised for revascularization with coronary artery bypass grafting (CABG).

Comments

In this patient, the LAD territory visually showed normal uptake, although the RCA and LCX territories showed severe ischemia. Since the normalization of the perfusion images were performed with the highest uptake voxel being regarded as normal, myocardial segments with higher uptake than the rest of the LV would visually appear to have normal uptake despite being, themselves, ischemic.

MBF values can demonstrate subnormal stress flow in myocardial segments that appear normal, and can suggest the presence of inducible ischemia and related coronary stenosis. This is particularly helpful in balanced ischemia that is related to multi-vessel disease in which all coronary arteries are similarly stenosed and there is uniform, but low global perfusion that may appear, visually, as normal. Post-stress LV dilatation and low MBF are the only indications of ischemia in such cases. In this particular case, the severe ischemia in the RCA and LCX territories were visually apparent, but the LAD involvement was determined on MBF estimation.

Conclusion

This study illustrated the value of a PET/CT MBF estimation to help determine the presence of ischemia in myocardial segments that appear visually normal in the presence of severe ischemia in adjacent segments. ■

Examination Protocol

Scanner: Biograph mCT

PET	
Injected Dose	40 mCi (1480 MBq) ^{82}Rb
Scan Delay	Immediate acquisition
Acquisition	Dynamic list mode
CT	Low-dose, free-breathing attenuation correction
Tube Voltage	120 kV
Tube Current	30 mAs
Slice Collimator	3 mm
Slice Thickness	5 mm

Case 6

Detection of Single Vessel Coronary Artery Disease with ^{82}Rb PET/CT Myocardial Perfusion Study

By Nimish Dhruva, MD

Data courtesy of Piedmont Heart, Atlanta, GA, USA

History

A 63-year-old man with longstanding diabetes and hypertension presented with complaints of occasional chest pain. The patient underwent a stress/rest ^{82}Rb myocardial perfusion PET/CT study, performed with a Biograph™ mCT scanner. Dynamic list mode acquisition was started immediately following infusion of 40 mCi (1480 MBq) of ^{82}Rb during regadenoson stress. Dynamic stress acquisition was continued for 7 minutes. Using an identical protocol, the rest acquisition was performed soon after the stress study.

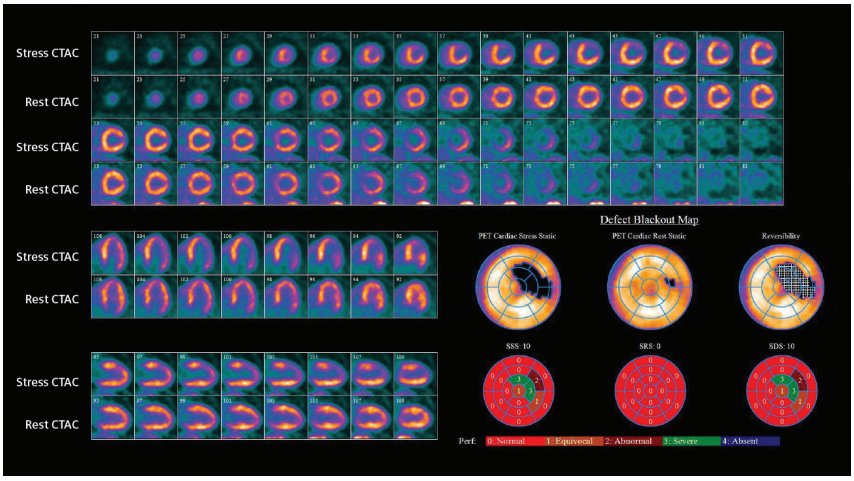

Figure 1: Stress/rest ^{82}Rb PET/CT MPI shows a severe, but reversible perfusion defect in the anterolateral wall, adjacent to the apex.

Diagnosis

The ^{82}Rb PET/CT myocardial perfusion study showed a severe, but completely reversible perfusion defect in the anterolateral wall, adjacent to the apex. The apex showed absence of ischemia. The anterior wall, septum and inferior wall showed normal per-

fusion. Post-stress transient ischemic dilatation of the left ventricle (LV) was also evident. The study suggested a reversible anterolateral ischemia, sparing the apex, which was possibly related to a stenosis of a big diagonal branch of the left anterior descending (LAD) or possibly a mid-LAD stenosis.

The patient subsequently underwent a coronary angiography. The coronary angiogram (*Figure 2*) showed a 70% stenosis in the proximal LAD (*arrows*). The D1 is occluded and fills by collateral. Left circumflex (LCX) and right coronary artery (RCA) were normal. Patient was advised revascularization.

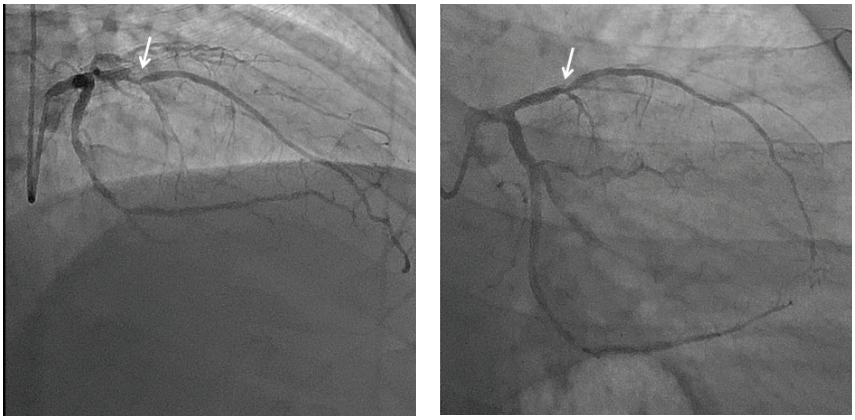

Figure 2: A coronary angiogram shows stenosis of proximal LAD (*arrows*).

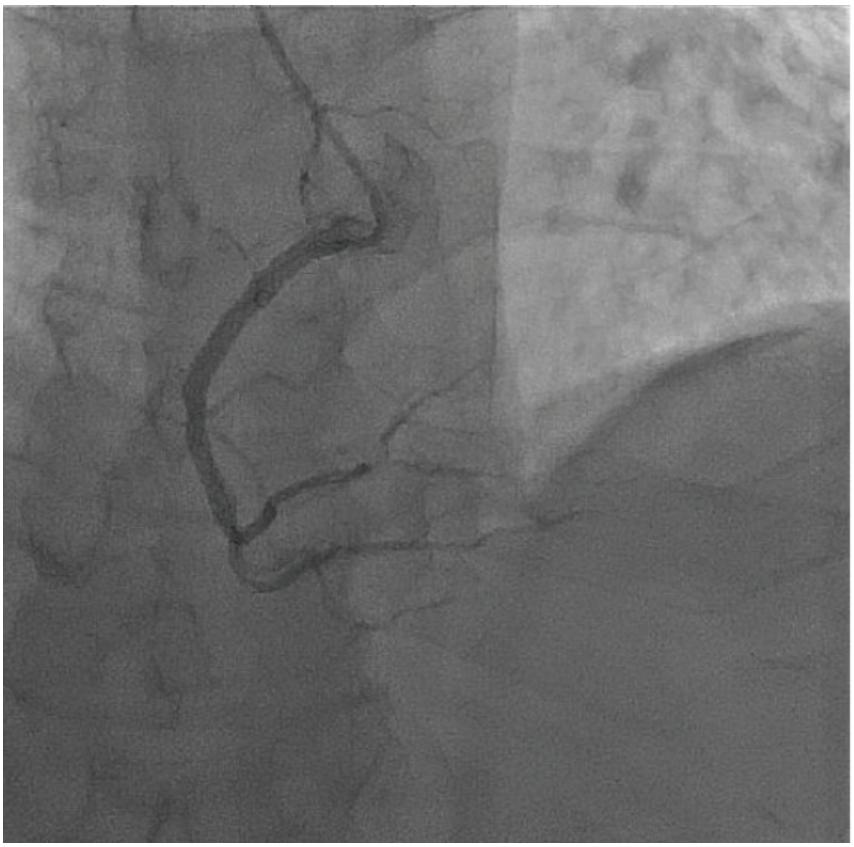

Figure 3: The RCA appears normal on coronary angiography.

Comments

The pattern of ischemia correlated perfectly with the angiogram results. Proximal LAD and D1 stenosis led to severe anterolateral, while the septum, apex, inferior and inferolateral walls were spared. The limited area of ischemia and the predominant anterolateral location of the ischemic zone suggested a single vessel disease, possibly a D1 or mid-LAD lesion.

Conclusion

PET/CT myocardial perfusion accurately depicted the limited ischemic segment, thereby helping to predict the culprit vessel and stenosis location. Although the lesion involved a single coronary artery, the transient ischemic dilatation possibly reflected stress-induced ischemic myocardial dysfunction in a large part of the LV, LAD being the dominant vessel supplying more than half of the LV. ■

Examination Protocol

Scanner: Biograph mCT

PET	
Injected Dose	40 mCi (1480 MBq) ^{82}Rb
Scan Delay	Immediate acquisition
Acquisition	Dynamic list mode
CT	
Tube Voltage	120 kV
Tube Current	30 mAs
Slice Collimation	3 mm
Slice Thickness	5 mm

The statements by Siemens customers described herein are based on results that were achieved in the customer's unique setting. Since there is no "typical" hospital and many variables exist (e.g., hospital size, case mix, level of IT adoption) there can be no guarantee that other customers will achieve the same results.

Case 7

Characterization of Pericardial Metastases from Carcinoid Tumor Using ^{18}F FDG* PET/MR

By Ihn Ho Cho, MD; and Eun Jung Kong, MD

Data courtesy of the Department of Nuclear Medicine, Yeungnam University Hospital, Daegu, South Korea

History

A 36-year-old man with a biopsy-proven rectal carcinoid tumor underwent a Fludeoxyglucose F 18 (^{18}F FDG) PET/CT for evaluation of metastases. The PET/CT demonstrated a solitary hyper-metabolic mass in the lateral wall of the heart, which was suspicious for a pericardial metastasis. But myocardial invasion could not be ruled out. No other metastatic lesion was demonstrated. To further characterize the pericardial mass, the patient was referred for ^{18}F FDG PET/MR, performed on Biograph™ mMR, using simultaneous acquisition of PET and MR.

The study was performed 1 hour following a 6.4 mCi (236 MBq) intravenous injection of ^{18}F FDG. Cardiac-gated resting PET acquisition was performed along with simultaneous acquisition of various MR sequences, including HASTE, TrueFISP Cine, T2 fat saturation.

Diagnosis

PET/MR images demonstrated a hyper-metabolic ovoid pericardial mass (3.8 x 2.2 cm) in the lateral wall of the left ventricle (LV), showing clear separation from the lateral wall myocardium and minimal pleural effusion (*Figure 1*).

T2 fat saturation images showed the pericardial mass to be slightly hyper-intense to that of the LV myocardium, but with a clear plane separating the mass from the normal LV myocardium (*Figure 2*). There was a small peripheral hypo-intense area on the T2 fat saturation image (*Figure 2, arrow*), which was related to intratumoral calcification and was visualized in a separately performed CT (*Figure 3*). Tissue characteristics of the myocardial masses were similar to those of the surrounding normal myocardium on TrueFISP Cine imaging.

The pericardial mass was adherent, but separate from the LV myocardium, and did not infiltrate into the LV lateral wall or papillary muscles (*Figure 4*). The signal void seen in the T2 fat saturation images (*Figure 2*) reflected the calcification (*Figure 3*). Hyper-intensity seen on the T1 fat saturation images (*Figure 4*), in the region of calcification, suggested the presence of additional tissue components. A histopathological evaluation of the tumor showed that the calcified portion of the mass, which also corresponded to the area of hyper-intensity of the T1 fat saturation, consisted of calcification and fibrosis. There were no malignant cells in the calcified portion. The absence of tumor cells within the enhancing area was confirmed by the absence of ^{18}F FDG uptake within the region of calcification, as seen in the fused PET/MR image (*Figure 1*).

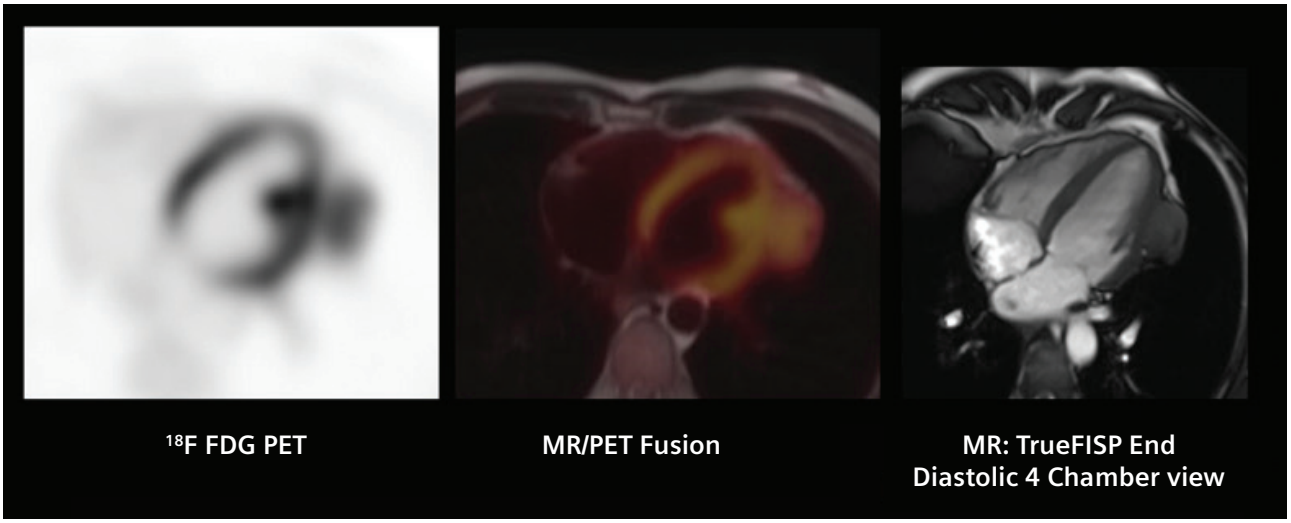

Figure 1: 4-chamber view of ^{18}F FDG PET, MR and PET/MR fusion shows a hyper-metabolic pericardial mass in the lateral wall of the LV.

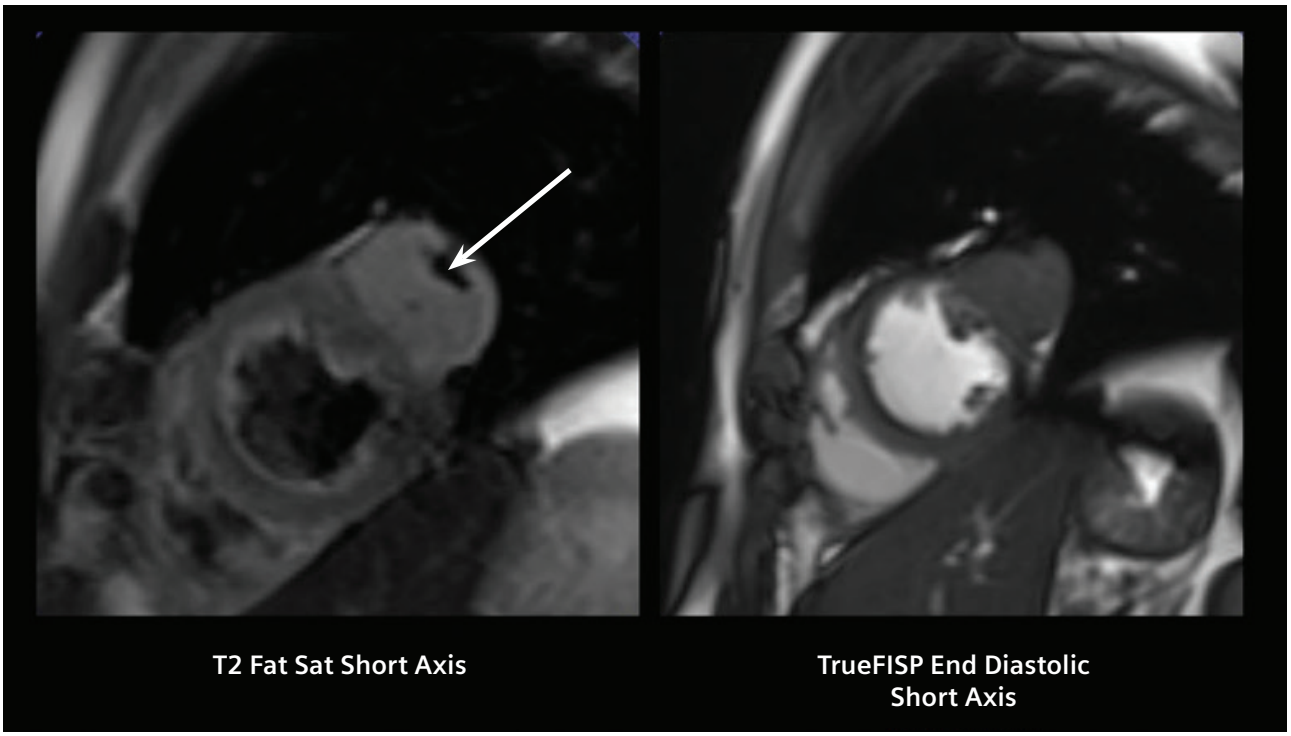

Figure 2: Short axis views of the T2 fat saturation show a pericardial mass in the lateral wall, which is slightly hyper-intense to the adjacent LV myocardium, but with clear margins between the normal myocardium and the pericardial mass. TrueFISP Cine short axis views show normal myocardial thickening without outflow obstruction or dyskinesia, which is due to the pericardial mass in the lateral LV wall.

The patient was referred for surgical excision of the pericardial mass. Surgery was performed under cardiopulmonary bypass through median sternotomy. A histopathological study of the excised mass revealed a carcinoid tumor. The final diagnosis was a metastatic neuroendocrine tumor involving pericardium of the lateral wall of the LV, originating from the primary rectal carcinoid.

The patient had an uneventful recovery and was on regular follow-up. Based on a CT performed 18 months post-surgery, there was no evidence of recurrence.

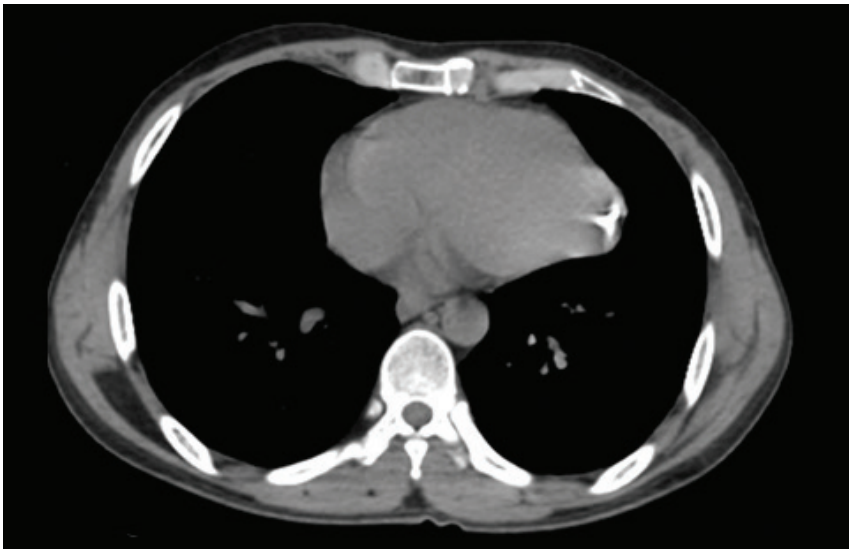

Figure 3: Separately performed non-contrast CT shows a cardiac mass in the lateral wall of the LV, containing focal areas of calcification.

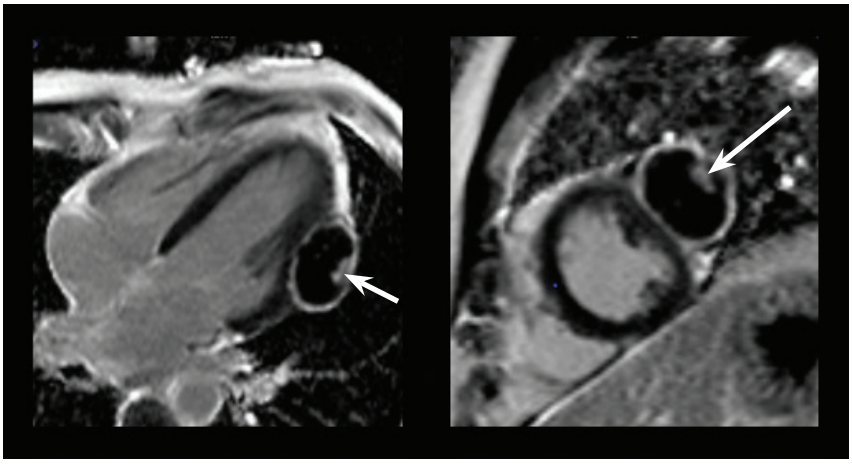

Figure 4: 4-chamber and short-axis views of T1 fat saturation show hypo-intensity of the pericardial mass with a hyper-intense peripheral rim.

Comments

Carcinoid tumors may be associated with cardiac involvement, with right-sided endocardial and valvular fibrous lesions of the heart.[1] This so-called carcinoid heart disease may present with cardiac failure and arrhythmias. Less commonly, myocardial metastases are diagnosed in carcinoid disease. Among patients with metastatic carcinoid disease, the overall incidence of myocardial metastases is about 4%.[2] These metastases usually are discovered during screening for distant metastatic disease, as in the present example, but may also present with arrhythmias.

^{18}F FDG avidity of the metastatic carcinoid tumor in the LV pericardium is probably related to a poorly differentiated aggressive tumor. High ^{18}F FDG uptake has been reported in bronchogenic carcinoids.[3] In these tumors, glucose transporter type 1 (GLUT-1) was expressed in a membranous pattern in the oncocytic component. Oncocytic carcinoid tumors could show intense ^{18}F FDG uptake due to the numerous intracellular mitochondria and the membranous overexpression of GLUT-1.[4] To the author's knowledge, no case report of ^{18}F FDG-avid cardiac metastases from carcinoid tumors exist.

MRI findings confirmed the absence of carcinoid heart disease since there was no valvular thickening, or abnormal valvular motion or ventricular dilatation, both of which are hallmarks of carcinoid heart disease.[5] MR findings helped characterize the tumor. The T2 fat saturation sequence helped to differentiate the tumor from normal myocardium, because the mass has higher signal intensity due to increased water content from the edema or inflammation.

Conclusion

Simultaneous acquisition of ^{18}F FDG PET and MR on Biograph mMR was instrumental in confirming the pericardial origin of the metastases from the rectal carcinoid, since on the fat suppression MR and the end diastolic PET, the mass could be clearly separated from the myocardium of the lateral wall of the LV. This was better defined on PET/MR due to the simultaneous acquisition of the MR and PET, so that there was exact co-registration of the pericardial mass defined by MR and the uptake in PET.

The decision for surgical excision of the pericardial metastases was based on the lack of infiltration into the LV myocardium by the mass that was clearly defined on PET/MR. Demonstration of infiltration of the LV myocardium would require a therapy choice, one between surgery or radiation therapy, based on the post-operative risk of papillary muscle injury or malignant arrhythmia. ■

Examination Protocol

Scanner: Biograph mMR

PET	
Injected Dose	6.4 mCi (236 MBq) ^{18}F FDG
Scan Delay	1 hr post-injection
Acquisition	List mode, gated; 1 bed position for 10 min
MR	Simultaneous MR acquisition
	HASTE breath hold
	TrueFISP Cine
	T1 Fat Saturation

References:
1 *Circulation*. 2007. 116: 2860 –2865.
2 *J Am Coll Cardiol* 2002, 40: 1328-1332.
3 *Thorax*. 2011, April. 66(4): 361-362.
4 *Ann Nucl Med*. 2013, Oct. 27(8): 781.
5 *Circ Cardiovasc Imaging*. 2010. 3: 103-111.

* The full prescribing information for the Fludeoxyglucose F 18 injection can be found on pages 42-44.

***Fludeoxyglucose F 18 5-10 mCi as an IV injection**

INDICATIONS AND USAGE

Fludeoxyglucose F 18 Injection (^{18}F FDG) is indicated for positron emission tomography (PET) imaging in the following settings:

- **Oncology:** For assessment of abnormal glucose metabolism to assist in the evaluation of malignancy in patients with known or suspected abnormalities found by other testing modalities, or in patients with an existing diagnosis of cancer.
- **Cardiology:** For the identification of left ventricular myocardium with residual glucose metabolism and reversible loss of systolic function in patients with coronary artery disease and left ventricular dysfunction, when used together with myocardial perfusion imaging.
- **Neurology:** For the identification of regions of abnormal glucose metabolism associated with foci of epileptic seizures.

IMPORTANT SAFETY INFORMATION

- **Radiation Risk**

  Radiation-emitting products, including Fludeoxyglucose F 18 Injection, may increase the risk for cancer, especially in pediatric patients. Use the smallest dose necessary for imaging and ensure safe handling to protect the patient and health care worker.

- **Blood Glucose Abnormalities**

  In the oncology and neurology setting, suboptimal imaging may occur in patients with inadequately regulated blood glucose levels. In these patients, consider medical therapy and laboratory testing to assure at least two days of normoglycemia prior to Fludeoxyglucose F 18 Injection administration.

- **Adverse Reactions**
  Hypersensitivity reactions with pruritus, edema and rash have been reported; have emergency resuscitation equipment and personnel immediately available.

- **Dosage Forms and Strengths**
  Multiple-dose 30 mL and 50 mL glass vial containing 0.74 to 7.40 GBq/mL (20 to 200 mCi/mL) of Fludeoxyglucose F 18 injection and 4.5 mg of sodium chloride with 0.1 to 0.5% w/w ethanolas a stabilizer (approximately 15 to 50 mL volume) for intravenous administration.

Full prescribing information for Fludeoxyglucose F 18 Injection can be found on pages 42-44.

Fludeoxyglucose F 18 injection is manufactured by Siemens' PETNET Solutions, 810 Innovation Drive, Knoxville, TN 39732

Case 8

Delineation of Severe Multi-vessel Coronary Artery Disease with IQ•SPECT

By Partha Ghosh, MD, Molecular Imaging Business Unit, Siemens Healthcare

Data courtesy of the Institute of Cardiology, Montreal, Canada

History
A 70-year-old male, who had diabetes, mild hypertension and a family history of coronary artery disease (CAD), presented with gradually progressive exertional dyspnea and occasional chest pain. The patient had been irregularly treated with anti-hypertensives and beta blockers without perfusion imaging or angiography. Because there was a likelihood of ischemia, the patient was referred for a ^{99m}Tc MIBI stress/rest myocardial perfusion study.

A 5-minute IQ•SPECT acquisition was performed on a Symbia™ T6 scanner, with 17 stops at 15 sec/stop, 1 hour following an IV injection of ^{99m}Tc MIBI (15 mCi [555 MBq]) at peak heart rate (85% of target heart rate) during treadmill exercise. A low-dose CT was performed for attenuation correction. The rest study was performed on the same day following an injection of ^{99m}Tc MIBI (35 mCi [1295 MBq]) with similar acquisition protocols using IQ•SPECT.

Diagnosis
Attenuation-corrected stress/rest IQ•SPECT myocardial perfusion images (*Figure 1*) showed a severe, but reversible perfusion defect in the anterior, apex, septum and antero-septal walls. This suggested severe, but reversible ischemia in the left anterior descending (LAD) territory. The inferior wall and inferolateral segment showed moderately decreased perfusion, with improved uptake in the rest study, pointing towards moderate and reversible ischemia. The lateral and posterolateral walls also showed a similar level of moderate reversible ischemia.

The resting images showed slightly decreased uptake in the anterior wall and apex, which reflected resting ischemia and correlates with advanced disease. The left ventricle (LV) showed significant dilatation, both in stress and rest images. The overall impression from the study was of reversible global ischemia with severe ischemia in the LAD territory. The clinical impression was of multi-vessel disease, with the most severe lesion in the LAD. Resting LV dilatation also reflected severe ischemia and advanced disease with impaired myocardial contractility, even at rest.

In view of the IQ•SPECT's detection of severe ischemia, the patient underwent coronary angiography. Subsequently, triple vessel disease was revealed. The angiography showed 90% proximal and mid-LAD stenosis, 90% stenosis of proximal right coronary artery (RCA) and diffuse mid left circumflex (LCX) stenosis. Because of both the angiography and IQ•SPECT discovery of global reversibility, the patient was advised for coronary bypass surgery.

Comments
This case was a typical example of multi-vessel CAD, with predominant involvement of 1 or 2 coronary

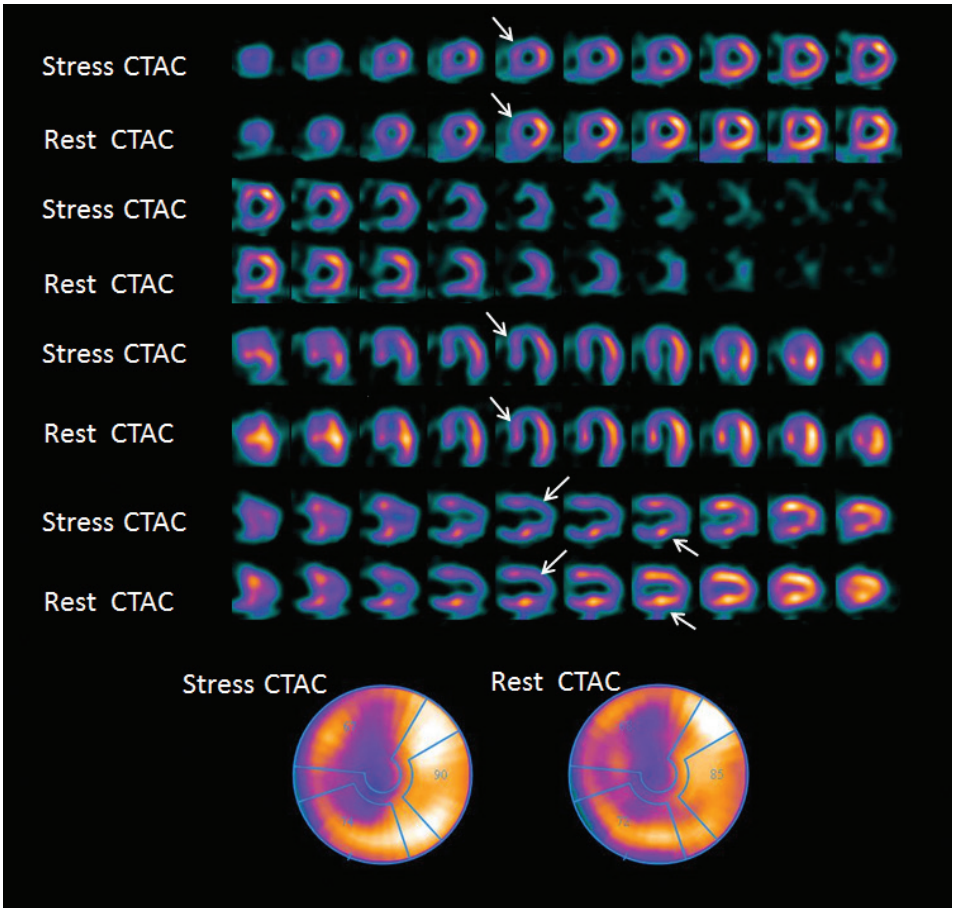

Figure 1: Stress/rest IQ•SPECT myocardial perfusion study shows reversible global ischemia with severe perfusion defects in the anterior and septum walls.

arteries. In this example, severe LAD territory ischemia coexisted with moderate ischemia in the RCA and LCX territories. The severity of LAD territory ischemia involving a large part of the LV resulted in a resting perfusion defect and LV dilatation at rest, all of which reflects hibernating myocardium due to presence of reversibility in the grossly ischemic anterior and septum walls. With complete reversibility seen in all 3 arterial territories, revascularization would lead to substantial increase in LV contractility and ejection fraction.

Conclusion

Despite the short, 5-minute acquisition time, IQ•SPECT clearly defined the degree of inducible ischemia and reversibility in all arterial territories, along with ventricular dilatation for optimum diagnostic evaluation and management decision making. ■

Examination Protocol

Scanner: Symbia T6

SPECT	
Injected Dose	Stress, 15 mCi (555 Mbq); rest, 35 mCi (1295 MBq) ^{99m}Tc MIBI
Scan Delay	60 min
Scan Speed	17 stops, 15 sec/stop
Acquisition	5-min IQ•SPECT (stress/rest)

CT	Low-dose attenuation correction
Tube Voltage	130 kV
Tube Current	30 mAs
Slice Collimation	3 mm
Slice Thickness	5 mm

The statements by Siemens customers described herein are based on results that were achieved in the customer's unique setting. Since there is no "typical" hospital and many variables exist (e.g., hospital size, case mix, level of IT adoption) there can be no guarantee that other customers will achieve the same results.

Case 9

Detection of Global Ischemia by IQ•SPECT in Patient with Suspected Coronary Artery Disease

By Partha Ghosh, MD, Molecular Imaging Business Unit, Siemens Healthcare

Data courtesy of the Institute of Cardiology, Montreal, Canada

History
A 63-year-old obese male with a history of diabetes presented with complaints of occasional shortness of breath upon exertion. The symptoms were mild, usually precipitating after the patient had climbed several flights of stairs and, with rest, promptly subsided. Therefore, the patient was referred for a ^{99m}Tc MIBI stress/rest myocardial perfusion SPECT/CT study to evaluate for the presence of inducible ischemia.

Since the patient was unlikely to exercise, a dipyridamole stress was performed. One hour following an IV injection of ^{99m}Tc MIBI (12 mCi [444 MBq]), a 4-minute IQ•SPECT acquisition was conducted on a Symbia™ T6 scanner. A low-dose CT was performed for attenuation correction. The rest study was performed on the same day following an injection of ^{99m}Tc MIBI (30 mCi [1110 MBq]) with similar acquisition protocols using IQ•SPECT.

Diagnosis
Attenuation-corrected stress/rest myocardial perfusion images (*Figure 1*) showed a moderate reversible perfusion defect in the inferior and inferolateral walls, suggesting reversible ischemia in the right coronary artery (RCA) territory. There was significant post-stress dilatation of the left ventricle (LV), with normal LV dimension at rest. Transient ischemic dilatation of that nature suggested moderate global ischemia, which in turn, pointed towards multi-vessel coronary artery disease (CAD)—though the reversible ischemia was predominantly in the inferior, anterior and septum walls. The lateral and posterolateral walls showed normal tracer uptake.

In view of the myocardial perfusion study, the patient was subjected to coronary angiography.

Coronary angiography revealed 90% proximal RCA stenosis with 70% stenosis of proximal LAD and OM1. The angiographic findings correlated well with the SPECT/CT findings, which demonstrated moderate global ischemia with predominant involvement of the RCA territory. As such, the patient was advised angioplasty of all 3 stenosis, with stenting of the RCA lesion.

Comments
This study demonstrates the definition of multi-vessel CAD by IQ•SPECT based on evaluation of stress-induced transient ischemic dilatation of the LV along with visualization of reversible ischemia in the RCA territory. The moderate nature of the global ischemia was reflected by the relatively well-preserved uptake in the LAD and left circumflex (LCX) territories at peak stress.

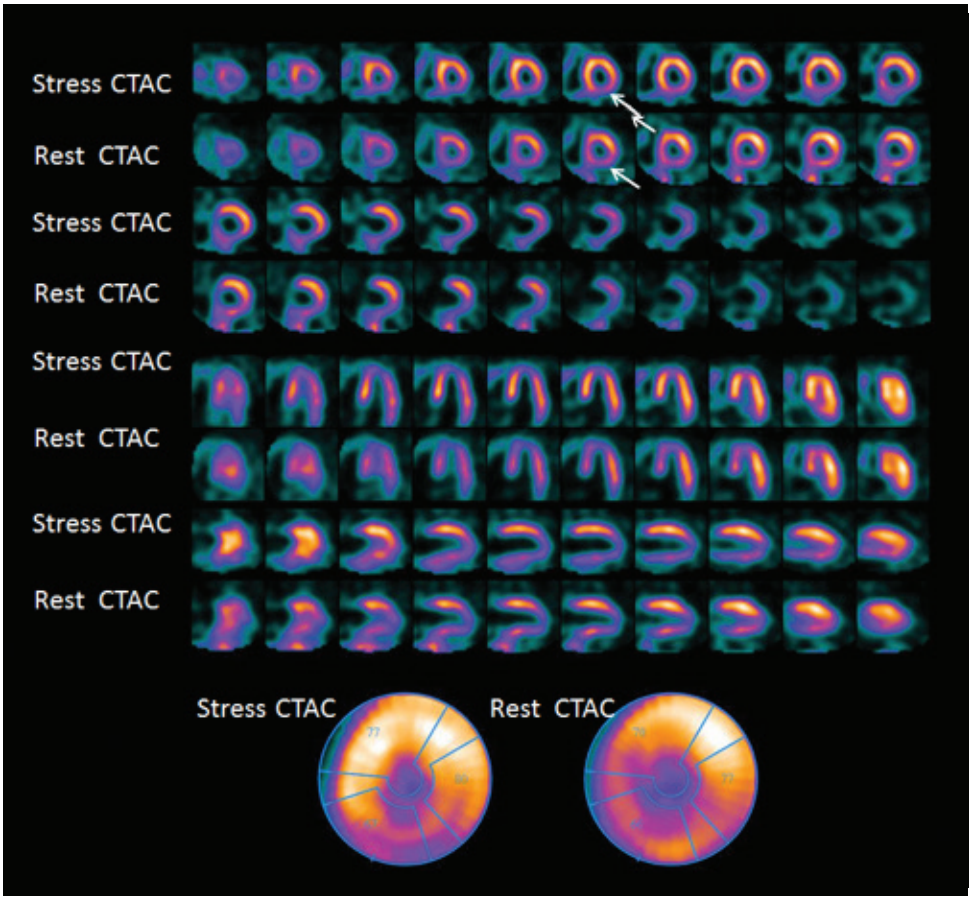

Figure 1: Attenuation-corrected stress and rest myocardial perfusion images show decreased perfusion at stress in the inferior and inferolateral walls, with moderate reversibility.

Conclusion

Attenuation-corrected IQ•SPECT not only defines perfusion defects and reversibility in individual coronary artery territories adequately, but it can also demonstrate subtle changes in LV dimensions following stress in order to identify clinically significant transient ischemic dilatation. With only a 4-minute acquisition for both stress and rest studies, IQ•SPECT on Symbia T6 provided a comprehensive evaluation of myocardial perfusion with robust attenuation correction. ■

Examination Protocol

Scanner: Symbia T6

SPECT	
Injected Dose	Stress, 12 mCi (444 MBq); rest, 30 mCi (1110 MBq) ^{99m}Tc MIBI
Scan Delay	60 min
Acquisition	4-min IQ•SPECT (stress/rest); 17 stops, 11 sec/stop
CT	Low-dose attenuation correction
Tube Voltage	130 kV
Tube Current	30 mAs
Slice Collimation	3 mm
Slice Thickness	5 mm

The statements by Siemens' customers described herein are based on results that were achieved in the customer's unique setting. Since there is no "typical" hospital and many variables exist (e.g., hospital size, case mix level of IT adoption) there can be no guarantee that other customers will achieve the same results.

Case 10

Delineation of Subtle Ischemia with ^{201}Tl Myocardial Perfusion Study Using IQ•SPECT in a Patient with Mitral Regurgitation

By K. Nakajima, MD; S. Matsuo, MD; and T. Konishi, RT

Data courtesy of Kanazawa University Hospital, Kanazawa, Japan

History

A 60-year-old woman, who had a history of coronary artery disease (CAD) that was treated with coronary artery bypass grafting (CABG) and an aortic aneurysm that was operated 3 years prior, presented with severe mitral valve regurgitation. A stress/rest Thallium-201 (^{201}Tl) myocardial perfusion study was performed for preoperative evaluation for mitral valve replacement surgery. The study was performed on a Symbia™ T6 scanner using IQ•SPECT. 74 MBq (2 mCi) of ^{201}Tl were injected at peak stress during adenosine infusion. Using a protocol of 17 frames per head (34 total) with a dwell time of 14 sec per frame, the IQ•SPECT study was performed immediately following isotope administration. A low-dose CT (130 kV; 20 mAs; 5 mm slice thickness) was performed for attenuation correction. 3 hours following the initial injection, 37 MBq (1 mCi) of ^{201}Tl were reinjected, and the rest study was acquired using an identical protocol.

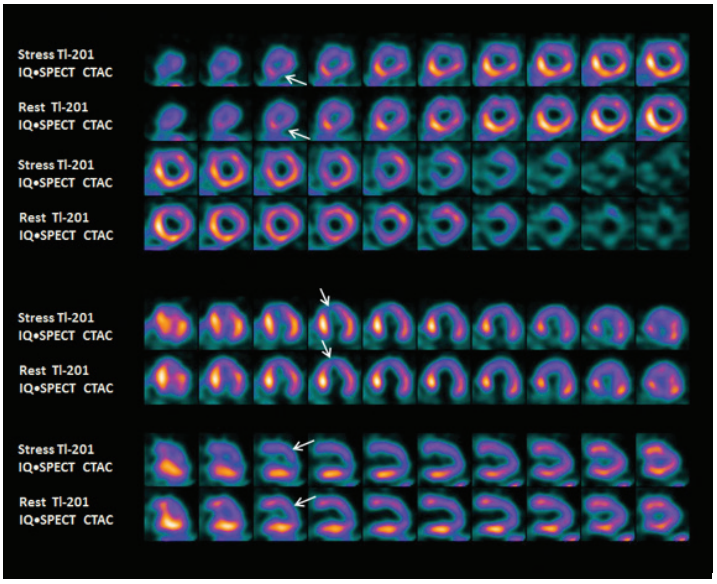

Figure 1: Stress/rest, attenuation-corrected ^{201}Tl IQ•SPECT myocardial perfusion study shows heterogeneous tracer distribution in the anterior wall and slight anterolateral ischemia near the apex.

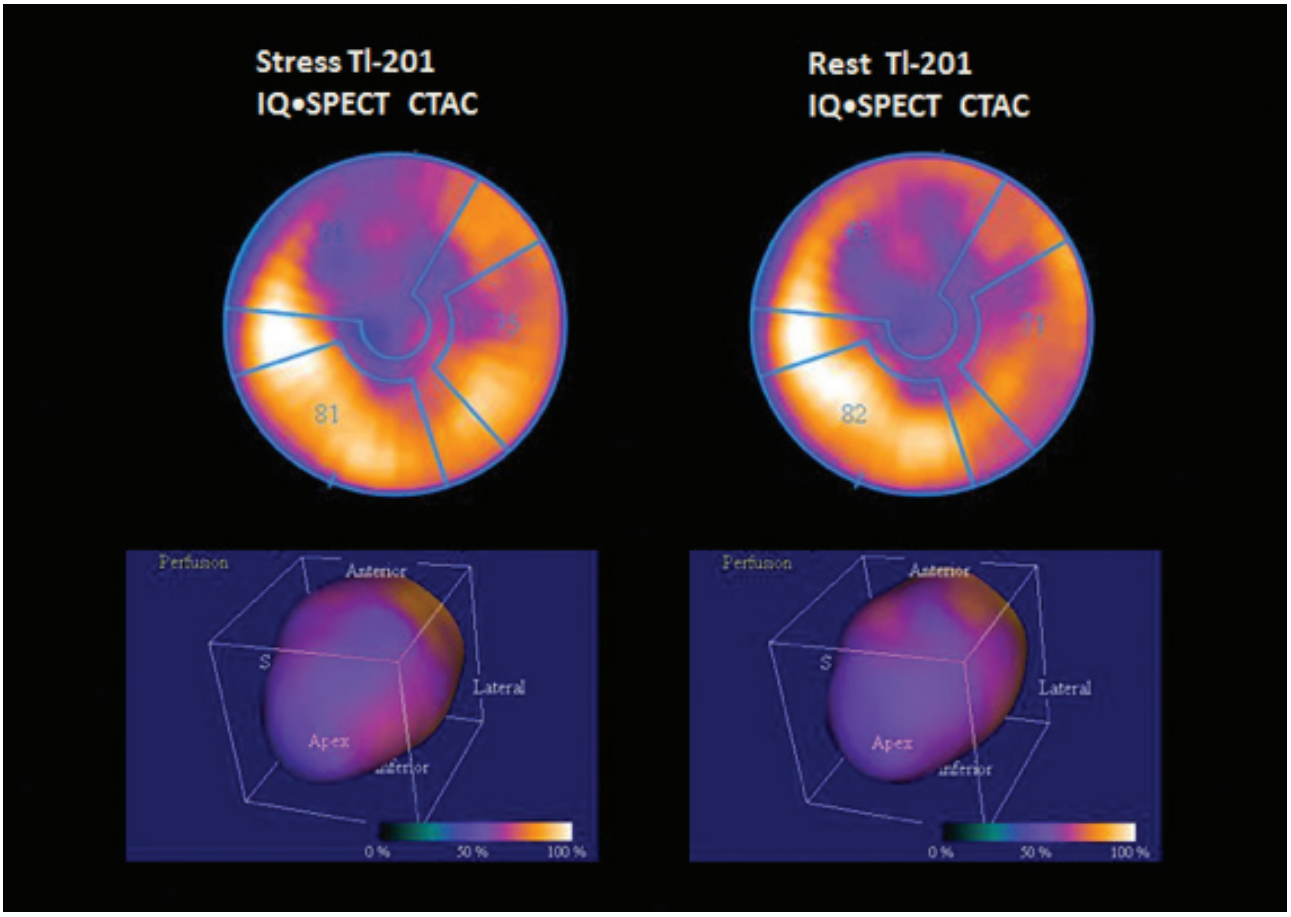

Figure 2: Bull's eye plot and volume rendering of the stress/rest perfusion show heterogenous tracer distribution in the anterior wall, lateral wall and apex.

Diagnosis
The ^{201}Tl IQ•SPECT myocardial perfusion study showed heterogenous distribution of tracer in the anterior wall, lateral wall and apex. Slight reversible ischemia is visualized in the anterolateral wall and adjacent apex. The left ventricle (LV) is dilated (EDV = 157 ml) with decreased LV contractility and low LV ejection fraction (LVEF) of 37%.

The patient underwent CT coronary angiography, which revealed bypass graft occlusion to right coronary artery (RCA) with flow to the RCA from the patent left anterior descending (LAD) coronary artery. The left circumflex (LCX) coronary artery was also patent.

Comments
The heterogenous uptake in the anterior wall and apex, and the LV dilatation and decreased contractility, probably reflect the long-standing mitral regurgitation with resulting ventricular dysfunction that is associated with the chronic decompensation phase of mitral regurgitation. The patient had a history of CABG with saphenous vein graft to the RCA, which was completely occluded. The slight anterolateral ischemia corresponded to the distal region of the LAD and/or LCX coronary artery. The limited area of ischemia in anterolateral wall reflects the fact that RCA is non-dominant, and there is good collateral flow from patent LAD and LCX coronary artery.

Conclusion
IQ•SPECT provides comprehensive evaluation of myocardial perfusion and ventricular function, even with a short scan time of 5 minutes along with CT attenuation correction. ■

Examination Protocol

Scanner: Symbia T6

SPECT	
Injected Dose	Stress, 74 MBq (2 mCi); rest, 37 MBq (1 mCi) ^{201}Tl
Acquisition	17 frames per head (34 total), 14 sec/frame
CT	
Tube Voltage	130 kV
Tube Current	20 mAs
Slice Collimation	3 mm
Slice Thickness	5 mm

The statements by Siemens' customers described herein are based on results that were achieved in the customer's unique setting. Since there is no "typical" hospital and many variables exist (e.g., hospital size, case mix level of IT adoption) there can be no guarantee that other customers will achieve the same results.

Case 11

Determination of Myocardial Perfusion and Viability Using ^{201}Tl and ^{123}I BMIPP Dual-isotope SPECT in a Patient with Multi-vessel Coronary Artery Disease

By K. Nakajima, MD; S. Matsuo, MD; and T. Konishi, RT

Data courtesy of Kanazawa University Hospital, Kanazawa, Japan

History

A 70-year-old male presented with gradually progressive shortness of breath during mild exertion and occasional chest pains. Coronary angiography revealed triple vessel disease with 100% occlusion of the proximal left anterior descending (LAD), 75% proximal stenosis of the left circumflex (LCX) and 90% proximal and mid-stenosis of the right coronary artery (RCA). To decide on the feasibility of revascularization (coronary artery bypass grafting [CABG]), the patient underwent a Thallium-201 (^{201}Tl) Iodine-123 (^{123}I) BMIPP dual-isotope SPECT study to assess resting myocardial perfusion and fatty acid metabolism in order to evaluate myocardial viability.

The study was performed on a Symbia™ T6 scanner immediately following an IV injection of 111 MBq (3 mCi) of ^{201}Tl and 111 MBq (3 mCi) of ^{123}I BMIPP. A gated SPECT study using a low-medium energy general purpose (LMEGP) collimator was performed with an acquisition protocol of 26 frames and 40 sec/frame. No CT acquisition was performed, since the studies were not corrected for attenuation.

Diagnosis

Dual-isotope study (*Figure 1 & 2*) showed resting ^{201}Tl perfusion, and the ^{123}I BMIPP fatty acid metabolism images showed severe and matching decreases in tracer uptake in the apex, apical anteroseptal and inferolateral and inferobasal walls. This suggested a severe resting perfusion deficit, secondary to long-standing coronary stenosis, along with absence of significant myocardial viability. There was, however, a small area in the lateral wall adjacent to the apex (*white arrows*) that showed perfusion-metabolism mismatch (slightly reduced perfusion in ^{201}Tl images, but further and severe decrease in ^{123}I BMIPP uptake suggesting significant mismatch), which reflected ischemic, but viable myocardium.

The main purpose of the study was to confirm the viability of LAD region. Considering the severe ^{201}Tl defect in the basal inferolateral wall, this region was judged as non-viable. The mid to basal anteroseptal wall (preserved perfusion and fatty acid metabolism) and small apical lateral wall (mismatched region) were judged as viable.

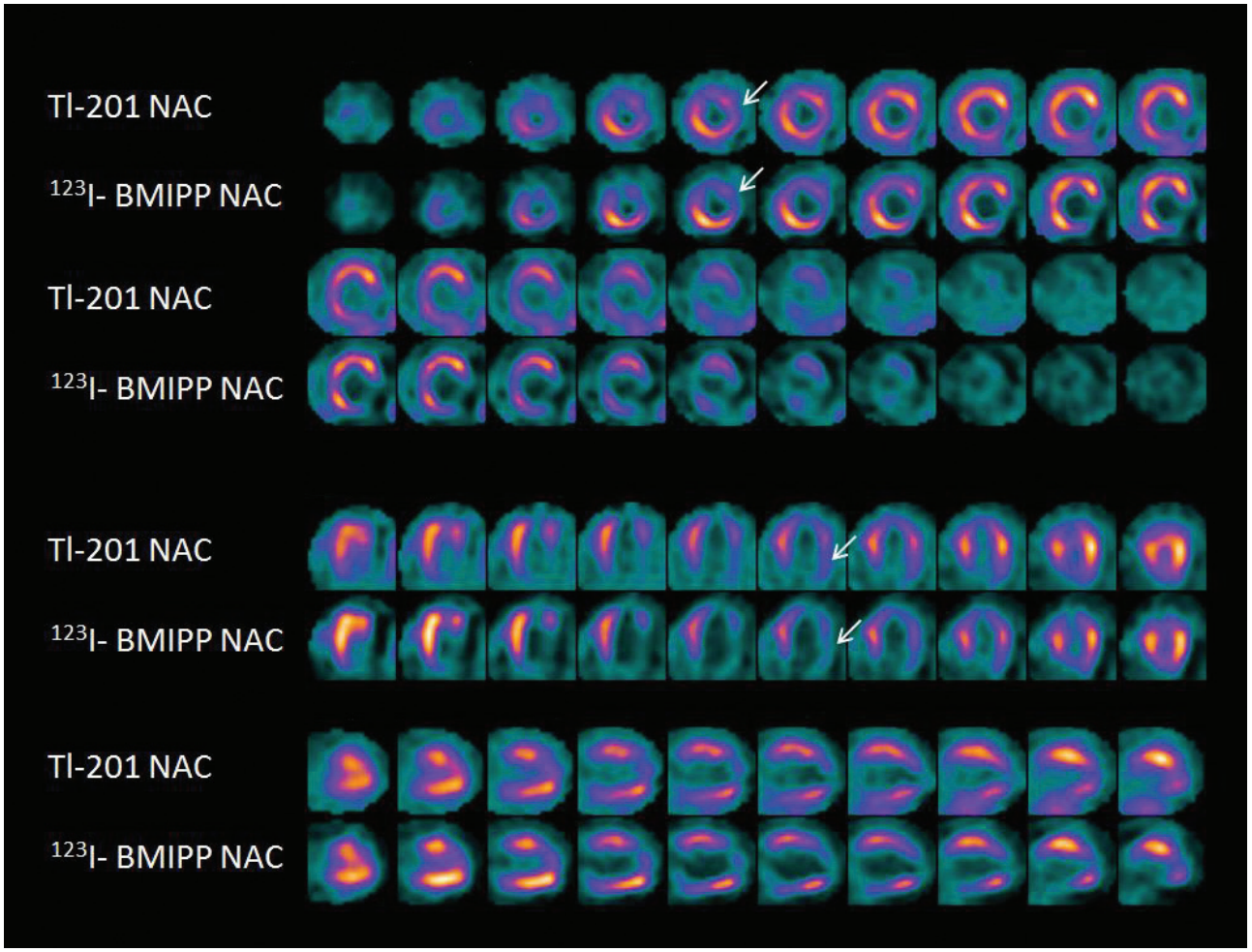

Figure 1: Resting dual-isotope study shows decreased ^{201}Tl and ^{123}I BMIPP uptake in the apex, anteroseptal, lateral and inferobasal walls. There is a small area of perfusion-metabolism mismatch in the lateral wall adjacent to apex (*arrows*). A matching severe defect was observed in mid to basal inferolateral walls.

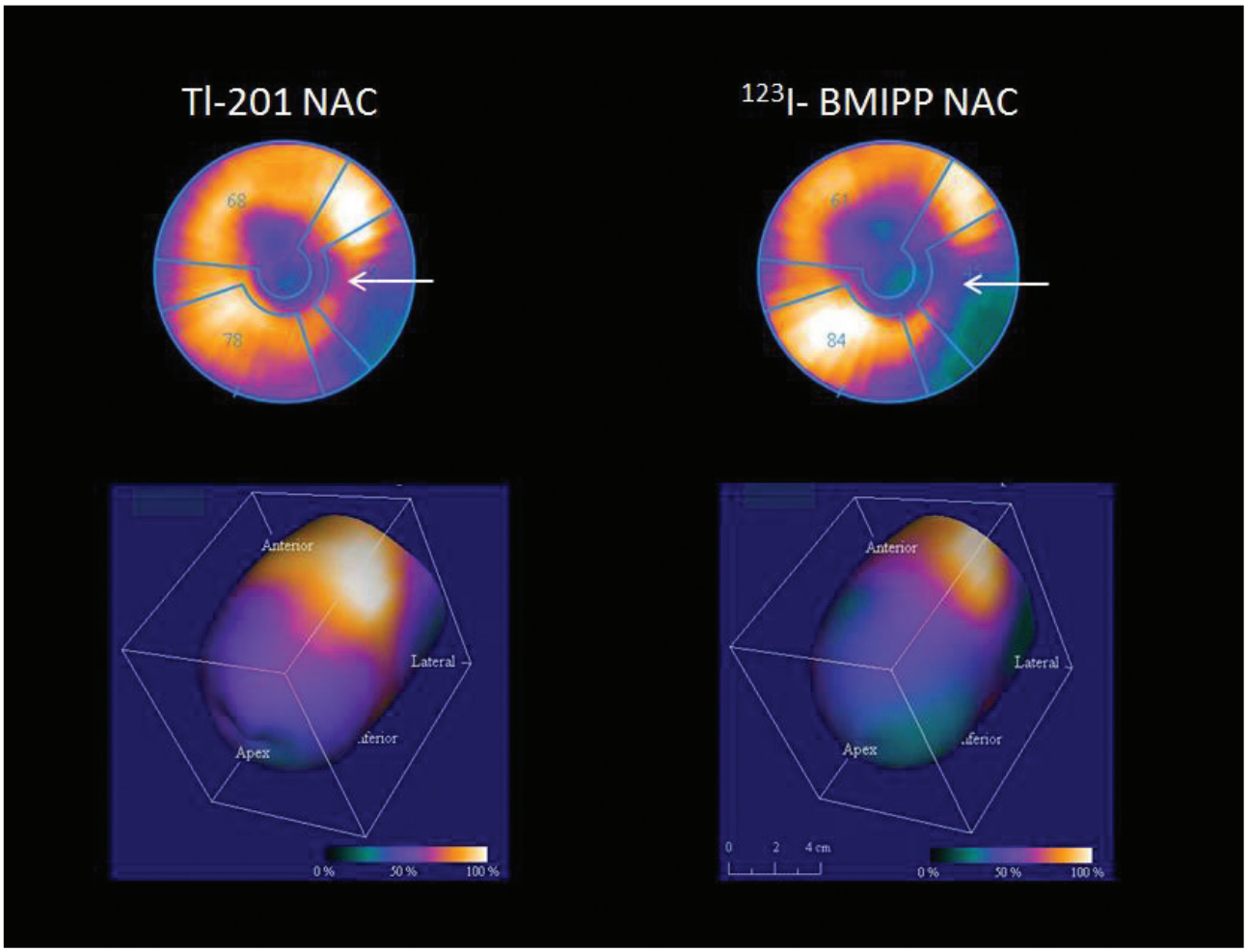

Figure 2: Bull's eye plot and volume rendering of resting ^{201}Tl perfusion and ^{123}I BMIPP fatty acid metabolism images show small area of perfusion-metabolism mismatch (*arrow*) in the lateral wall adjacent to apex, but with matching defects in the apical anterior wall, apex, and inferior and inferobasal walls.

The left ventricle (LV) was dilated with a high-end diastolic volume of 229 ml, along with markedly reduced resting LV ejection fraction (LVEF) of 25%. Such resting LV dilatation and low resting EF reflected severe myocardial dysfunction secondary to extensive myocardial scarring and gross resting ischemia and was an adverse prognostic indicator.

Although part of the lateral wall (the LCX) showed viability, the amount of viable myocardium was deemed too small compared to the large part of the LV myocardium, which showed matching defect and was labelled as non-viable. Thus, revascularization with CABG was not recommended in view of the predominance of non-viable myocardium. However, the indication might be considered for occluded LAD region.

Comments

Long-chain fatty acids are the principal energy source for a normally perfused myocardium. With ischemia, energy metabolism shifts to anaerobic metabolism, and the main energy substrate changes from free fatty acids (FFA) to glucose metabolism. Radiolabeled fatty acids like ^{123}I BMIPP can be used to image myocardial fatty acid metabolism, especially in situations of acute or chronic myocardial ischemic insult.

Myocardial metabolism shifts from FFA to glucose during acute ischemia and the resulting metabolic abnormality persists even after the perfusion returns to normal. This is common in episodes of myocardial stunning when acute ischemic episodes are usually followed by normal resting flow. Myocardial fatty acid metabolism remains decreased for a prolonged period of time in spite of normalization of resting perfusion, and thus, ^{123}I BMIPP imaging can detect previous ischemic insult, even after recovery of myocardial perfusion, the so called "ischemic memory."

Ischemic, but viable myocardial segments can be detected by identifying perfusion metabolism mismatch, where the decrease in ^{123}I BMIPP uptake is significantly lower than the perfusion. Dual-isotope imaging of ^{201}Tl myocardial perfusion and ^{123}I BMIPP is a useful tool. Since the principal energies of ^{201}Tl and ^{123}I vary, a dual-isotope acquisition is feasible. A matching defect shows similar levels of decrease in perfusion as well as fatty acid metabolism, which reflects a myocardial scar.

In this patient, the amount of matching defect (myocardial scar) was much larger than the small area in the lateral wall with a mismatch (suggestive of viability), which suggested revascularization may not lead to significant improvement in myocardial contractility, perfusion and LVEF. In long-standing, severe coronary stenosis, as in this patient, decrease in ^{123}I BMIPP uptake is mainly due to repeated ischemic episodes with delayed recovery of fatty acid metabolism.[1] These abnormalities may be due to a reduced coronary flow reserve (CFR) in the dysfunctional area.

In a study of chronic CAD, the severity of ^{123}I BMIPP uptake was found to be closely related to the reduction of CFR as assessed by quantitative ^{15}O-labelled water PET myocardial perfusion imaging.[2] ^{123}I BMIPP SPECT has proven useful as a prognostic indicator, and discordant BMIPP and ^{201}Tl uptake accurately predict functional recovery of myocardial function after revascularization. Fujita et al.[3] performed dual-isotope studies in 98 patients with CAD requiring CABG with a LVEF less than 50%. Patients who showed >5% improvement in LVEF following CABG had significantly higher perfusion-metabolism mismatch compared to those who failed to show improvement. The mismatch score was the best predictor of which patient would improve LVEF following revascularization. In the current patient, the amount of LV myocardium with mismatch was far smaller than the amount of myocardium with matching defects, which supports the prediction that CABG may not improve LV function.

Conclusion

This study illustrates the value of resting dual-isotope ^{201}Tl and ^{123}I BMIPP SPECT study in patients with advanced coronary artery disease (CAD) for assessment of resting myocardial perfusion and viability to support decision making for revascularization. ■

Examination Protocol

Scanner: Symbia T6

SPECT	
Injected Dose	111 MBq (3 mCi) ^{201}Tl; 111 MBq (3 mCi) ^{123}I BMIPP
Acquisition	26 frames, 40 sec/frame

References:

[1] Yoshinaga et al. *Eur J Nucl Med Mol Imaging*. 2014; 41: 384–393.

[2] Kageyama et al. *Eur J Nucl Med Mol* Imaging. 2006; 33: 6–12.

[3] Fujita et al. *Nucl Med Commun*. 2015 Feb; 36(2): 148-155.

Congresses & Events

2015/2016

Event	Date	Location	Event Website
Pacific Southwest Technologist Chapter, SNMMI	July 18, 2015	Las Vegas, NV, USA	*www.wrsnm.org*
American Association of Physicists in Medicine	July 12-16, 2015	Anaheim, CA, USA	*www.aapm.org*
European Society of Cardiology	August 29-September 5, 2015	London, England, UK	*www.escardio.org/ESC2015*
American Society of Nuclear Cardiology	September 17-20, 2015	Washington, DC, USA	*www.asnc.org*
Southeastern Chapter, SNMMI	October 2-4, 2015	Charleston, SC, USA	*www.secsnm.org*
International Conference on Clinical PET/CT and Molecular Imaging: PET/CT in the Era of Multimodality Imaging and Image-Guided Therapy	October 5-9, 2015	Vienna, Austria	*www-pub.iaea.org/iaeameetings*
Missouri Valley Chapter, SNMMI	October 9-11, 2015	St. Louis, MI, USA	*www.mvcsnm.org*
Central Chapter, SNMMI, Fall Education Symposium	October 10-11, 2015	Indianapolis, IN, USA	*www.ccsnmmi.org*
European Association of Nuclear Medicine	October 10-14, 2015	Hamburg, Germany	*www.eanm.org*
American Society for Therapeutic Radiology and Oncology, 57th Annual Meeting	October 11-12, 2015	San Antonio, TX, USA	*www.astro.org*
Western Regional Annual Meeting, SNMMI	October 22-25, 2015	Monterey, CA, USA	*www.wrsnm.org*
The 11th Asia Oceania Congress of Nuclear Medicine and Biology	October 31-November 4	Jeju, South Korea	*http://aocnmb2015.com/*

Congresses & Events (cont.)

2015/2016

Event	Date	Location	Event Website
Northeast Regional Meeting (New England/Greater New York Chapters, SNMMI)	November 6-7, 2015	Newport, RI, USA	*www.greaternycsnm.org/events.htm*
La Asociación Latinoamericana de Sociedades de Biología y Medicina Nuclear	November 18-21, 2015	Punta del Este, Uruguay	*www.alasbimn2015.org.uy/*
Radiological Society of North America	November 29-December 4, 2015	Chicago, IL, USA	*www.rsna.org*
Arab Health	January 25-28, 2016	Dubai, UAE	*www.arabhealthonline.com/*
SNMMI 2016 Mid-Winter Meeting	January 28-31, 2016	Orlando, FL, USA	*www.snmmi.org*
European Congress of Radiology	March 2-6, 2016	Vienna, Austria	*www.myesr.org*
European Molecular Imaging Meeting - EMIM 2016	March 8-10, 2016	Utrecht, the Netherlands	*www.e-smi.eu*
New England Chapter, SNMMI	April 8-9, 2016	Newport, RI, USA	*http://nects.org*
Mid-Eastern Chapter, SNMMI, 45th Annual Spring Meeting	April 15-17, 2016	Linthicum Heights, MA, USA	*www.mecsnm.net*
Nuklear Medizin 2016 (Germany Society of Nuclear Medicine)	April 20-23, 2016	Dresden, Germany	*www.nuklearmedizin.de/events*
European Society for Radiotherapy & Oncology	April 29-May 3, 2016	Turin, Italy	*www.estro.org*
Polish Society of Nuclear Medicine	June 1-4, 2016	Krakow, Poland	*www.ptnm.org*
Society of Nuclear Medicine Annual Meeting	June 11-15, 2016	San Diego, CA, USA	*www.snmmi.org*

Siemens Healthcare Customer Magazines

Our customer magazine family offers the latest information and background for every healthcare field. From the hospital director to the radiological assistant—here, you can quickly find information relevant to your needs.

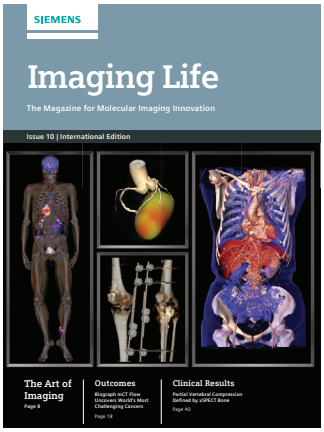

Imaging Life
Everything from the world of molecular imaging innovations.

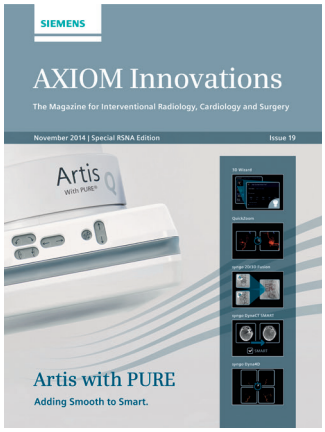

AXIOM Innovations
Everything from the world of interventional radiology, cardiology, and surgery.

Medical Solutions
Innovations and trends in healthcare. The magazine is designed especially for members of hospital management, administration personnel and heads of medical departments.

Scan and Subscribe!

For current and past issues and to order the magazines, please visit **siemens.com/healthcare-magazine**

MAGNETOM Flash
Everything from the world of magnetic resonance imaging.

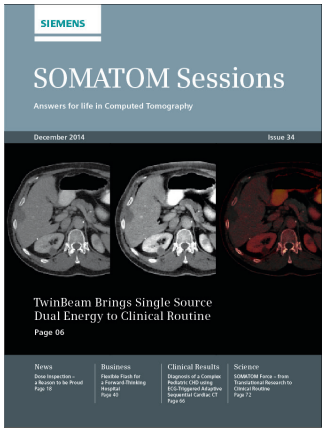

SOMATOM Sessions
Everything from the world of computed tomography.

Imaging Life magazines and articles are available for download online at: **siemens.com/imaginglife**

Publisher:
Siemens Medical Solutions USA, Inc.
Molecular Imaging
2501 North Barrington Road
Hoffman Estates, IL 60192
USA
Phone: +1 847 304-7700
siemens.com/mi

Editor: Rhett Morici
rhett.morici@siemens.com

Responsible for Content:
Partha Ghosh
partha.ghosh@siemens.com

Design Consulting:
Vieceli Design, Inc., Illinois, USA

Printer: Tewell Warren Printing,
Colorado, USA

Cover Image:
Data courtesy of CHU de Quèbec,
Quèbec City, Canada

Note in accordance with § 33 Para.1 of the German Federal Data Protection Law: Dispatch is made using an address file which is maintained with the aid of an automated data processing system.

We remind our readers that when printed, X-ray films never disclose all the information content of the original. Artifacts in CT, MR, SPECT, SPECT/CT, PET, PET/CT and PET/MR images are recognizable by their typical features and are generally distinguishable from existing pathology. As referenced below, healthcare practioners are expected to utilize their own learning, training and expertise in evaluating images.

Please contact your local Siemens sales representative for the most current information.

Note: Original images always lose a certain amount of detail when reproduced. All comparative claims derived from competitive data at the time of printing. Data on file.

The consent of the authors and publisher are required for the reprint or reuse of an article. Please contact Siemens for further information. Suggestions, proposals and information are always welcome; they are carefully examined and submitted to the editorial board for attention. Imaging Life is not responsible for loss, damage or any other injury to unsolicited manuscripts or materials.

We welcome your questions and comments about the editorial content of Imaging Life. Please contact us at imaginglife.healthcare@siemens.com.

Imaging Life is available on the internet: siemens.com/imaginglife

Imaging Life also has a free iPad and iPhone App available. From your iPad or iPhone, go to the App Store and search "Imaging Life," then download.

Some of the imaging biomarkers in this publication are not currently recognized by the U.S. Food and Drug Administration (FDA) or other regulatory agencies as being safe and effective, and Siemens does not make any claims regarding their use.

DISCLAIMERS: Imaging Life: "The information presented in this magazine is for illustration only and is not intended to be relied upon by the reader for instruction as to the practice of medicine. Healthcare practitioners reading this information are reminded that they must use their own learning, training and expertise in dealing with their individual patients. This material does not substitute for that duty and is not intended by Siemens Healthcare to be used for any purpose in that regard." Contrast Agents: "The drugs and doses mentioned herein are consistent with the approved labeling for uses and/or indications of the drug. The treating physician bears the sole responsibility for the diagnosis and treatment of patients, including drugs and doses prescribed in connection with such use. The Operating Instructions must always be strictly followed when operating your Siemens system. The source for the technical data is the corresponding data sheets." Trademarks: "All trademarks mentioned in this document are property of their respective owners." Results: "The outcomes achieved by the Siemens customers described herein were achieved in the customer's unique setting. Since there is no "typical" hospital and many variables exist (e.g., hospital size, case mix, level of IT adoption), there can be no guarantee that others will achieve the same results."

HIGHLIGHTS OF PRESCRIBING INFORMATION

These highlights do not include all the information needed to use Fludeoxyglucose F 18 Injection safely and effectively. See full prescribing information for Fludeoxyglucose F 18 Injection.

Fludeoxyglucose F 18 Injection, USP

For intravenous use

Initial U.S. Approval: 2005

RECENT MAJOR CHANGES

Warnings and Precautions (5.1, 5.2) 7/2010

Adverse Reactions (6) 7/2010

INDICATIONS AND USAGE

Fludeoxyglucose F18 Injection is indicated for positron emission tomography (PET) imaging in the following settings:

- Oncology: For assessment of abnormal glucose metabolism to assist in the evaluation of malignancy in patients with known or suspected abnormalities found by other testing modalities, or in patients with an existing diagnosis of cancer.
- Cardiology: For the identification of left ventricular myocardium with residual glucose metabolism and reversible loss of systolic function in patients with coronary artery disease and left ventricular dysfunction, when used together with myocardial perfusion imaging.
- Neurology: For the identification of regions of abnormal glucose metabolism associated with foci of epileptic seizures (1).

DOSAGE AND ADMINISTRATION

Fludeoxyglucose F 18 Injection emits radiation. Use procedures to minimize radiation exposure. Screen for blood glucose abnormalities.

- In the oncology and neurology settings, instruct patients to fast for 4 to 6 hours prior to the drug's injection. Consider medical therapy and laboratory testing to assure at least two days of normoglycemia prior to the drug's administration (5.2).
- In the cardiology setting, administration of glucose-containing food or liquids (e.g., 50 to 75 grams) prior to the drug's injection facilitates localization of cardiac ischemia (2.3).

Aseptically withdraw Fludeoxyglucose F 18 Injection from its container and administer by intravenous injection (2).

The recommended dose:

- for adults is 5 to 10 mCi (185 to 370 MBq), in all indicated clinical settings (2.1).
- for pediatric patients is 2.6 mCi in the neurology setting (2.2).

Initiate imaging within 40 minutes following drug injection; acquire static emission images 30 to 100 minutes from time of injection (2).

DOSAGE FORMS AND STRENGTHS

Multi-dose 30mL and 50mL glass vial containing 0.74 to 7.40 GBq/mL (20 to 200 mCi/mL) Fludeoxyglucose

F 18 Injection and 4.5mg of sodium chloride with 0.1 to 0.5% w/w ethanol as a stabilizer (approximately 15 to 50 mL volume) for intravenous administration (3).

CONTRAINDICATIONS

None

WARNINGS AND PRECAUTIONS

- Radiation risks: use smallest dose necessary for imaging (5.1).
- Blood glucose adnormalities: may cause suboptimal imaging (5.2).

ADVERSE REACTIONS

Hypersensitivity reactions have occurred; have emergency resuscitation equipment and personnel immediately available (6).

To report SUSPECTED ADVERSE REACTIONS, contact PETNET Solutions, Inc. at 877-473-8638 or FDA at 1-800-FDA-1088 or www.fda.gov/medwatch.

USE IN SPECIFIC POPULATIONS

Pregnancy Category C: No human or animal data. Consider alternative diagnostics; use only if clearly needed (8.1).

- Nursing mothers: Use alternatives to breast feeding (e.g., stored breast milk or infant formula) for at least 10 half-lives of radioactive decay, if Fludeoxyglucose F 18 Injection is administered to a woman who is breast-feeding (8.3).
- Pediatric Use: Safety and effectiveness in pediatric patients have not been established in the oncology and cardiology settings (8.4).

See 17 for PATIENT COUNSELING INFORMATION

Revised: 1/2011

FULL PRESCRIBING INFORMATION: CONTENTS*

* Sections or subsections omitted from the full prescribing information are not listed.

FULL PRESCRIBING INFORMATION

1 INDICATIONS AND USAGE

Fludeoxyglucose F 18 Injection is indicated for positron emission tomography (PET) imaging in the following settings:

1.1 Oncology

For assessment of abnormal glucose metabolism to assist in the evaluation of malignancy in patients with known or suspected abnormalities found by other testing modalities, or in patients with an existing diagnosis of cancer.

1.2 Cardiology

For the identification of left ventricular myocardium with residual glucose metabolism and reversible loss of systolic function in patients with coronary artery disease and left ventricular dysfunction, when used together with myocardial perfusion imaging.

1.3 Neurology

For the identification of regions of abnormal glucose metabolism associated with foci of epileptic seizures.

2 DOSAGE AND ADMINISTRATION

Fludeoxyglucose F 18 Injection emits radiation. Use procedures to minimize radiation exposure. Calculate the final dose from the end of synthesis (EOS) time using proper radioactive decay factors. Assay the final dose in a properly calibrated dose calibrator before administration to the patient [see Description (11.2)].

2.1 Recommended Dose for Adults

Within the oncology, cardiology and neurology settings, the recommended dose for adults is 5 to 10 mCi (185 to 370 MBq) as an intravenous injection.

2.2 Recommended Dose for Pediatric Patients

Within the neurology setting, the recommended dose for pediatric patients is 2.6 mCi, as an intravenous injection. The optimal dose adjustment on the basis of body size or weight has not been determined [see Use in Special Populations (8.4)].

2.3 Patient Preparation

- To minimize the radiation absorbed dose to the bladder, encourage adequate hydration. Encourage the patient to drink water or other fluids (as tolerated) in the 4 hours before their PET study.
- Encourage the patient to void as soon as the imaging study is completed and as often as possible thereafter for at least one hour.
- Screen patients for clinically significant blood glucose abnormalities by obtaining a history and/or laboratory tests [see Warnings and Precautions (5.2)]. Prior to Fludeoxyglucose F 18 PET imaging in the oncology and neurology settings, instruct patient to fast for 4 to 6 hours prior to the drug's injection.
- In the cardiology setting, administration of glucose-containing food or liquids (e.g., 50 to 75 grams) prior to Fludeoxyglucose F18 Injection facilitates localization of cardiac ischemia

2.4 Radiation Dosimetry

The estimated human absorbed radiation doses (rem/mCi) to a newborn (3.4 kg), 1-year old (9.8 kg), 5-year old (19 kg), 10-year old (32 kg), 15-year old (57 kg), and adult (70 kg) from intravenous administration of Fludeoxyglucose F 18 Injection are shown in Table 1. These estimates were calculated based on human[2] data and using the data published by the International Commission on Radiological Protection[4] for Fludeoxyglucose ^{18}F. The dosimetry data show that there are slight variations in absorbed radiation dose for various organs in each of the age groups. These dissimilarities in absorbed radiation dose are due to developmental age variations (e.g., organ size, location, and overall metabolic rate for each age group). The identified critical organs (in descending order) across all age groups evaluated are the urinary bladder, heart, pancreas, spleen, and lungs.

Table 1. Estimated Absorbed Radiation Doses (rem/mCi) After Intravenous Administration of Fludeoxyglucose F-18 Injection[a]

Organ	Newborn (3.4 kg)	1-year old (9.8 kg)	5-year old (19 kg)	10-year old (32 kg)	15-year old (57 kg)	Adult (70 kg)
Bladder wall[b]	4.3	1.7	0.93	0.60	0.40	0.32
Heart wall	2.4	1.2	0.70	0.44	0.29	0.22
Pancreas	2.2	0.68	0.33	0.25	0.13	0.096
Spleen	2.2	0.84	0.46	0.29	0.19	0.14
Lungs	0.96	0.38	0.20	0.13	0.092	0.064
Kidneys	0.81	0.34	0.19	0.13	0.089	0.074
Ovaries	0.80	0.8	0.19	0.11	0.058	0.053
Uterus	0.79	0.35	0.19	0.12	0.076	0.062
LLI wall *	0.69	0.28	0.15	0.097	0.060	0.051
Liver	0.69	0.31	0.17	0.11	0.076	0.058
Gallbladder wall	0.69	0.26	0.14	0.093	0.059	0.049
Small intestine	0.68	0.29	0.15	0.096	0.060	0.047
ULI wall **	0.67	0.27	0.15	0.090	0.057	0.046
Stomach wall	0.65	0.27	0.14	0.089	0.057	0.047
Adrenals	0.65	0.28	0.15	0.095	0.061	0.048
Testes	0.64	0.27	0.14	0.085	0.052	0.041
Red marrow	0.62	0.26	0.14	0.089	0.057	0.047
Thymus	0.61	0.26	0.14	0.086	0.056	0.044
Thyroid	0.61	0.26	0.13	0.080	0.049	0.039
Muscle	0.58	0.25	0.13	0.078	0.049	0.039
Bone surface	0.57	0.24	0.12	0.079	0.052	0.041
Breast	0.54	0.22	0.11	0.068	0.043	0.034
Skin	0.49	0.20	0.10	0.060	0.037	0.030
Brain	0.29	0.13	0.09	0.078	0.072	0.070
Other tissues	0.59	0.25	0.13	0.083	0.052	0.042

[a] MIRDOSE 2 software was used to calculate the radiation absorbed dose. Assumptions on the biodistribution based on data from Gallagher et al.1 and Jones et al.2

[b] The dynamic bladder model with a uniform voiding frequency of 1.5 hours was used. *LLI = lower large intestine; **ULI = upper large intestine

2.5 Radiation Safety – Drug Handling

- Use waterproof gloves, effective radiation shielding, and appropriate safety measures when handling Fludeoxyglucose F 18 Injection to avoid unnecessary radiation exposure to the patient, occupational workers, clinical personnel and other persons.
- Radiopharmaceuticals should be used by or under the control of physicians who are qualified by specific training and experience in the safe use and handling of radionuclides, and whose experience and training have been approved by the appropriate governmental agency authorized to license the use of radionuclides.
- Calculate the final dose from the end of synthesis (EOS) time using proper radioactive decay factors. Assay the final dose in a properly calibrated dose calibrator before administration to the patient [see Description (11.2)].
- The dose of Fludeoxyglucose F 18 used in a given patient should be minimized consistent with the objectives of the procedure, and the nature of the radiation detection devices employed.

2.6 Drug Preparation and Administration

- Calculate the necessary volume to administer based on calibration time and dose.
- Aseptically withdraw Fludeoxyglucose F 18 Injection from its container.
- Inspect Fludeoxyglucose F 18 Injection visually for particulate matter and discoloration before administration, whenever solution and container permit.
- Do not administer the drug if it contains particulate matter or discoloration; dispose of these unacceptable or unused preparations in a safe manner, in compliance with applicable regulations.
- Use Fludeoxyglucose F 18 Injection within 12 hours from the EOS.

2.7 Imaging Guidelines

- Initiate imaging within 40 minutes following Fludeoxyglucose F 18 Injection administration.
- Acquire static emission images 30 to 100 minutes from the time of injection.

3 DOSAGE FORMS AND STRENGTHS

Multiple-dose 30 mL and 50 mL glass vial containing 0.74 to 7.40 GBq/mL (20 to 200 mCi/mL) of Fludeoxyglucose F 18 Injection and 4.5 mg of sodium chloride with 0.1 to 0.5% w/w ethanol as a stabilizer (approximately 15 to 50 mL volume) for intravenous administration.

4 CONTRAINDICATIONS

None

5 WARNINGS AND PRECAUTIONS

5.1 Radiation Risks

Radiation-emitting products, including Fludeoxyglucose F 18 Injection, may increase the risk for cancer, especially in pediatric patients. Use the smallest dose necessary for imaging and ensure safe handling to protect the patient and health care worker [see Dosage and Administration (2.5)].

5.2 Blood Glucose Abnormalities

In the oncology and neurology setting, suboptimal imaging may occur in patients with inadequately regulated blood glucose levels. In these patients, consider medical therapy and laboratory testing to assure at least two days of normoglycemia prior to Fludeoxyglucose F 18 Injection administration.

6 ADVERSE REACTIONS

Hypersensitivity reactions with pruritus, edema and rash have been reported in the post-marketing setting. Have emergency resuscitation equipment and personnel immediately available.

7 DRUG INTERACTIONS

The possibility of interactions of Fludeoxyglucose F 18 Injection with other drugs taken by patients undergoing PET imaging has not been studied.

8 USE IN SPECIFIC POPULATIONS

8.1 Pregnancy

Pregnancy Category C

Animal reproduction studies have not been conducted with Fludeoxyglucose F 18 Injection. It is also not known whether Fludeoxyglucose F 18 Injection can cause fetal harm when administered to a pregnant woman or can affect reproduction capacity. Consider alternative diagnostic tests in a pregnant woman; administer Fludeoxyglucose F 18 Injection only if clearly needed.

8.3 Nursing Mothers

It is not known whether Fludeoxyglucose F 18 Injection is excreted in human milk. Consider alternative diagnostic tests in women who are breast-feeding. Use alternatives to breast feeding (e.g., stored breast milk or infant formula) for at least 10 half-lives of radioactive decay, if Fludeoxyglucose F 18 Injection is administered to a woman who is breast-feeding.

8.4 Pediatric Use

The safety and effectiveness of Fludeoxyglucose F 18 Injection in pediatric patients with epilepsy is established on the basis of studies in adult and pediatric patients. In pediatric patients with epilepsy, the recommended dose is 2.6 mCi. The optimal dose adjustment on the basis of body size or weight has not been determined. In the oncology or cardiology settings, the safety and effectiveness of Fludeoxyglucose F 18 Injection have not been established in pediatric patients.

11 DESCRIPTION

11.1 Chemical Characteristics

Fludeoxyglucose F 18 Injection is a positron emitting radiopharmaceutical that is used for diagnostic purposes in conjunction with positron emission tomography (PET) imaging. The active ingredient 2-deoxy-2-[^{18}F]fluoro-D-glucose has the molecular formula of $C_6H_{11}{}^{18}FO_5$ with a molecular weight of 181.26, and has the following chemical structure:

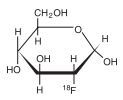

Fludeoxyglucose F 18 Injection is provided as a ready to use sterile, pyrogen free, clear, colorless solution. Each mL contains between 0.740 to 7.40GBq (20.0 to 200 mCi) of 2-deoxy-2-[^{18}F]fluoro-D-glucose at the EOS, 4.5 mg of sodium chloride and 0.1 to 0.5% w/w ethanol as a stabilizer. The pH of the solution is between 4.5 and 7.5. The solution is packaged in a multiple-dose glass vial and does not contain any preservative.

11.2 Physical Characteristics

Fluorine F 18 decays by emitting positron to Oxygen O 16 (stable) and has a physical half-life of 109.7 minutes. The principal photons useful for imaging are the dual 511 keV gamma photons, that are produced and emitted simultaneously in opposite direction when the positron interacts with an electron (Table 2).

Table 2. Pricipal Radiation Emission Data for Fluorine F18

Radiation/Emission	% Per Disintegration	Mean Energy
Positron (b+)	96.73	249.8 keV
Gamma (±)*	193.46	511.0 keV

*Produced by positron annihilation

From: Kocher, D.C. Radioactive Decay Tables DOE/TIC-I 1026, 89 (1981)

The specific gamma ray constant (point source air kerma coefficient) for fluorine F 18 is 5.7 R/hr/mCi (1.35 x 10-6 Gy/hr/kBq) at 1 cm. The half-value layer (HVL) for the 511 keV photons is 4 mm lead (Pb). The range of attenuation coefficients for this radionuclide as a function of lead shield thickness is shown in Table 3. For example, the interposition of an 8 mm thickness of Pb, with a coefficient of attenuation of 0.25, will decrease the external radiation by 75%.

Table 3. Radiation Attenuation of 511 keV Photons by lead (Pb) shielding

Shield thickness (Pb) mm	Coefficient of attenuation
0	0.00
4	0.50
8	0.25
13	0.10
26	0.01
39	0.001
52	0.0001

For use in correcting for physical decay of this radionuclide, the fractions remaining at selected intervals after calibration are shown in Table 4.

Table 4. Physical Decay Chart for Fluorine F18

Minutes	Fraction Remaining
0*	1.000
15	0.909
30	0.826
60	0.683
110	0.500
220	0.250

*calibration time

12 CLINICAL PHARMACOLOGY

12.1 Mechanism of Action

Fludeoxyglucose F 18 is a glucose analog that concentrates in cells that rely upon glucose as an energy source, or in cells whose dependence on glucose increases under pathophysiological conditions. Fludeoxyglucose F 18 is transported through the cell membrane by facilitative glucose transporter proteins and is phosphorylated within the cell to [^{18}F] FDG-6-phosphate by the enzyme hexokinase. Once phosphorylated it cannot exit until it is dephosphorylated by glucose-6-phosphatase. Therefore, within a given tissue or pathophysiological process, the retention and clearance of Fludeoxyglucose F 18 reflect a balance involving glucose transporter, hexokinase and glucose-6-phosphatase activities. When allowance is made for the kinetic differences between glucose and Fludeoxyglucose F 18 transport and phosphorylation (expressed as the ‚lumped constant" ratio), Fludeoxyglucose F 18 is used to assess glucose metabolism.

In comparison to background activity of the specific organ or tissue type, regions of decreased or absent uptake of Fludeoxyglucose F 18 reflect the decrease or absence of glucose metabolism. Regions of increased uptake of Fludeoxyglucose F 18 reflect greater than normal rates of glucose metabolism.

12.2 Pharmacodynamics

Fludeoxyglucose F 18 Injection is rapidly distributed to all organs of the body after intravenous administration. After background clearance of Fludeoxyglucose F 18 Injection, optimal PET imaging is generally achieved between 30 to 40 minutes after administration.

In cancer, the cells are generally characterized by enhanced glucose metabolism partially due to (1) an increase in activity of glucose transporters, (2) an increased rate of phosphorylation activity, (3) a reduction of phosphatase activity or, (4) a dynamic alteration in the balance among all these processes. However, glucose metabolism of cancer as reflected by Fludeoxyglucose F 18 accumulation shows considerable variability. Depending on tumor type, stage, and location, Fludeoxyglucose F 18 accumulation may be increased, normal, or decreased. Also, inflammatory cells can have the same variability of uptake of Fludeoxyglucose F 18.

In the heart, under normal aerobic conditions, the myocardium meets the bulk of its energy requirements by oxidizing free fatty acids. Most of the exogenous glucose taken up by the myocyte is converted into glycogen. However, under ischemic conditions, the oxidation of free fatty acids decreases, exogenous glucose becomes the preferred myocardial sub strate, glycolysis is stimulated, and glucose taken up by the myocyte is metabolized immediately instead of being converted into glycogen. Under these condi-

tions, phosphorylated Fludeoxyglucose F 18 accumulates in the myocyte and can be detected with PET imaging.

In the brain, cells normally rely on aerobic metabolism. In epilepsy, the glucose metabolism varies. Generally, during a seizure, glucose metabolism increases. Interictally, the seizure focus tends to be hypometabolic.

12.3 Pharmacokinetics

Distribution: In four healthy male volunteers, receiving an intravenous administration of 30 seconds in duration, the arterial blood level profile for Fludeoxyglucose F 18 decayed triexponentially. The effective half-life ranges of the three phases were 0.2 to 0.3 minutes, 10 to 13 minutes with a mean and standard deviation (STD) of 11.6 (±) 1.1 min, and 80 to 95 minutes with a mean and STD of 88 (±) 4 min.

Plasma protein binding of Fludeoxyglucose F 18 has not been studied.

Metabolism: Fludeoxyglucose F 18 is transported into cells and phosphorylated to [^{18}F]-FDG-6- phosphate at a rate proportional to the rate of glucose utilization within that tissue. [F18]-FDG-6-phosphate presumably is metabolized to 2-deoxy-2-[F18]fluoro-6-phospho-D-mannose([F 18]FDM-6-phosphate).

Fludeoxyglucose F 18 Injection may contain several impurities (e.g., 2-deoxy-2-chloro-D-glucose (ClDG)). Biodistribution and metabolism of ClDG are presumed to be similar to Fludeoxyglucose F 18 and would be expected to result in intracellular formation of 2-deoxy-2-chloro-6-phospho-D-glucose (ClDG-6-phosphate) and 2-deoxy-2-chloro-6-phospho-D-mannose (ClDM-6-phosphate). The phosphorylated deoxyglucose compounds are dephosphorylated and the resulting compounds (FDG, FDM, ClDG, and ClDM) presumably leave cells by passive diffusion. Fludeoxyglucose F 18 and related compounds are cleared from non-cardiac tissues within 3 to 24 hours after administration. Clearance from the cardiac tissue may require more than 96 hours. Fludeoxyglucose F 18 that is not involved in glucose metabolism in any tissue is then excreted in the urine.

Elimination: Fludeoxyglucose F 18 is cleared from most tissues within 24 hours and can be eliminated from the body unchanged in the urine. Three elimination phases have been identified in the reviewed literature. Within 33 minutes, a mean of 3.9% of the administrated radioactive dose was measured in the urine. The amount of radiation exposure of the urinary bladder at two hours post-administration suggests that 20.6% (mean) of the radioactive dose was present in the bladder.

Special Populations:

The pharmacokinetics of Fludeoxyglucose F 18 Injection have not been studied in renally-impaired, hepatically impaired or pediatric patients. Fludeoxyglucose F 18 is eliminated through the renal system. Avoid excessive radiation exposure to this organ system and adjacent tissues.

The effects of fasting, varying blood sugar levels, conditions of glucose intolerance, and diabetes mellitus on Fludeoxyglucose F 18 distribution in humans have not been ascertained [see Warnings and Precautions (5.2)].

13 NONCLINICAL TOXICOLOGY

13.1 Carcinogenesis, Mutagenesis, Impairment of Fertility

Animal studies have not been performed to evaluate the Fludeoxyglucose F 18 Injection carcinogenic potential, mutagenic potential or effects on fertility.

14 CLINICAL STUDIES

14.1 Oncology

The efficacy of Fludeoxyglucose F 18 Injection in positron emission tomography cancer imaging was demonstrated in 16 independent studies. These studies prospectively evaluated the use of Fludeoxyglucose F 18 in patients with suspected or known malignancies, including non-small cell lung cancer, colo-rectal, pancreatic, breast, thyroid, melanoma, Hodgkin's and non-Hodgkin's lymphoma, and various types of metastatic cancers to lung, liver, bone, and axillary nodes. All these studies had at least 50 patients and used pathology as a standard of truth. The Fludeoxyglucose F 18 Injection doses in the studies ranged from 200 MBq to 740 MBq with a median and mean dose of 370 MBq.

In the studies, the diagnostic performance of Fludeoxyglucose F 18 Injection varied with the type of cancer, size of cancer, and other clinical conditions. False negative and false positive scans were observed. Negative Fludeoxyglucose F 18 Injection PET scans do not exclude the diagnosis of cancer. Positive Fludeoxyglucose F 18 Injection PET scans can not replace pathology to establish a diagnosis of cancer. Non-malignant conditions such as fungal infections, inflammatory processes and benign tumors have patterns of increased glucose metabolism that may give rise to false-positive scans. The efficacy of Fludeoxyglucose F 18 Injection PET imaging in cancer screening was not studied.

14.2 Cardiology

The efficacy of Fludeoxyglucose F 18 Injection for cardiac use was demonstrated in ten independent, prospective studies of patients with coronary artery disease and chronic left ventricular systolic dysfunction who were scheduled to undergo coronary revascularization. Before revascularization, patients underwent PET imaging with Fludeoxyglucose F 18 Injection (74 to 370 MBq, 2 to 10 mCi) and perfusion imaging with other diagnostic radiopharmaceuticals. Doses of Fludeoxyglucose F 18 Injection ranged from 74 to 370 MBq (2 to 10 mCi). Segmental, left ventricular, wall-motion assessments of asynergic areas made before revascularization were compared in a blinded manner to assessments made after successful revascularization to identify myocardial segments with functional recovery.

Left ventricular myocardial segments were predicted to have reversible loss of systolic function if they showed Fludeoxyglucose F 18 accumulation and reduced perfusion (i.e., flow-metabolism mismatch). Conversely, myocardial segments were predicted to have irreversible loss of systolic function if they showed reductions in both Fludeoxyglucose F 18 accumulation and perfusion (i.e., matched defects).

Findings of flow-metabolism mismatch in a myocardial segment may suggest that successful revascularization will restore myocardial function in that segment. However, false-positive tests occur regularly, and the decision to have a patient undergo revascularization should not be based on PET findings alone. Similarly, findings of a matched defect in a myocardial segment may suggest that myocardial function will not recover in that segment, even if it is successfully revascularized. However, false-negative tests occur regularly, and the decision to recommend against coronary revascularization, or to recommend a cardiac transplant, should not be based on PET findings alone. The reversibility of segmental dysfunction as predicted with Fludeoxyglucose F 18 PET imaging depends on successful coronary revascularization. Therefore, in patients with a low likelihood of successful revascularization, the diagnostic usefulness of PET imaging with Fludeoxyglucose F 18 Injection is more limited.

14.3 Neurology

In a prospective, open label trial, Fludeoxyglucose F 18 Injection was evaluated in 86 patients with epilepsy. Each patient received a dose of Fludeoxyglucose F 18 Injection in the range of 185 to 370 MBq (5 to 10 mCi). The mean age was 16.4 years (range: 4 months to 58 years; of these, 42 patients were less than 12 years and 16 patients were less than 2 years old). Patients had a known diagnosis of complex partial epilepsy and were under evaluation for surgical treatment of their seizure disorder. Seizure foci had been previously identified on ictal EEGs and sphenoidal EEGs. Fludeoxyglucose F 18 Injection PET imaging confirmed previous diagnostic findings in 16% (14/87) of the patients; in 34% (30/87) of the patients, Fludeoxyglucose F 18 Injection PET images provided new findings. In 32% (27/87), imaging with Fludeoxyglucose F 18 Injection was inconclusive. The impact of these imaging findings on clinical outcomes is not known.

Several other studies comparing imaging with Fludeoxyglucose F 18 Injection results to subsphenoidal EEG, MRI and/or surgical findings supported the concept that the degree of hypometabolism corresponds to areas of confirmed epileptogenic foci. The safety and effectiveness of Fludeoxyglucose F 18 Injection to distinguish idiopathic epileptogenic foci from tumors or other brain lesions that may cause seizures have not been established.

15 REFERENCES

1. Gallagher B.M., Ansari A., Atkins H., Casella V., Christman D.R., Fowler J.S., Ido T., MacGregor R.R., Som P., Wan C.N., Wolf A.P., Kuhl D.E., and Reivich M. "Radiopharmaceuticals XXVII. 18F-labeled 2-deoxy-2-fluoro-d-glucose as a radiopharmaceutical for measuring regional myocardial glucose metabolism in vivo: tissue distribution and imaging studies in animals," J Nucl Med, 1977; 18, 990-6.
2. Jones S.C., Alavi, A., Christman D., Montanez, I., Wolf, A.P., and Reivich M. "The radiation dosimetry of 2 [F-18] fluoro-2-deoxy-D-glucose in man," J Nucl Med, 1982; 23, 613-617.
3. Kocher, D.C. "Radioactive Decay Tables: A handbook of decay data for application to radiation dosimetry and radiological assessments," 1981, DOE/TIC-I 1026, 89.
4. ICRP Publication 53, Volume 18, No. I-4,1987, pages 75-76.

16 HOW SUPPLIED/STORAGE AND DRUG HANDLING

Fludeoxyglucose F 18 Injection is supplied in a multi-dose, capped 30 mL and 50 mL glass vial containing between 0.740 to 7.40 GBq/mL (20 to 200 mCi/mL), of no carrier added 2-deoxy-2-[F 18] fluoro-D-glucose, at end of synthesis, in approximately 15 to 50 mL. The contents of each vial are sterile, pyrogen-free and preservative-free.

NDC 40028-511-30; 40028-511-50

Receipt, transfer, handling, possession, or use of this product is subject to the radioactive material regulations and licensing requirements of the U.S. Nuclear Regulatory Commission, Agreement States or Licensing States as appropriate.

Store the Fludeoxyglucose F 18 Injection vial upright in a lead shielded container at 25°C (77°F); excursions permitted to 15-30°C (59-86°F).

Store and dispose of Fludeoxyglucose F 18 Injection in accordance with the regulations and a general license, or its equivalent, of an Agreement State or a Licensing State.

The expiration date and time are provided on the container label. Use Fludeoxyglucose F 18 Injection within 12 hours from the EOS time.

17 PATIENT COUNSELING INFORMATION

Instruct patients in procedures that increase renal clearance of radioactivity. Encourage patients to:

- drink water or other fluids (as tolerated) in the 4 hours before their PET study.
- void as soon as the imaging study is completed and as often as possible thereafter for at least one hour.

Manufactured by: PETNET Solutions Inc.
810 Innovation Drive
Knoxville, TN 37932

Distributed by: PETNET Solutions Inc.
810 Innovation Drive
Knoxville, TN 37932

PETNET Solutions

PN0002262 Rev. A
March 1, 2011

On account of certain regional limitations of sales rights and service availability, we cannot guarantee that all products included in this brochure are available through the Siemens sales organization worldwide. Availability and packaging may vary by country and is subject to change without prior notice. Some/All of the features and products described herein may not be available in the United States.

The information in this document contains general technical descriptions of specifications and options as well as standard and optional features which do not always have to be present in individual cases.

Siemens reserves the right to modify the design, packaging, specifications and options described herein without prior notice.

Please contact your local Siemens sales representative for the most current information.

Note: Any technical data contained in this document may vary within defined tolerances. Original images always lose a certain amount of detail when reproduced.

Global Business Unit
Siemens Medical Solutions USA, Inc.
Molecular Imaging
2501 North Barrington Road
Hoffman Estates, IL 60192
USA
Phone: +1 847 304-7700
siemens.com/mi

Siemens Healthcare Headquarters
Siemens Healthcare GmbH
Henkestraße 127
91052 Erlangen
Germany
Phone: +49 9131 84-0
siemens.com/healthcare

Order No. A91MI-10424-T1-7600 | Printed in USA | MI-2351.RM.JV.TW.1M

siemens.com/imaginglife